JMEPEG (2004) 13:7-23
DOI: 10.1361/10599490417533

1059-9495/$19.00

# General and Localized Corrosion of Magnesium Alloys: A Critical Review

*Edward Ghali, Wolfgang Dietzel, and Karl-Ulrich Kainer*

*(Submitted 4 June 2003)*

**Magnesium (Mg) alloys as well as experimental alloys are emerging as light structural materials for current, new, and innovative applications. This paper describes the influence of the alloying elements and the different casting processes on the microstructure and performance of these alloys and corrosion. It gives a comprehensible approach for the resistance of these alloys to general, localized and metallurgically influenced corrosion, which are the main challenges for their use. Exposure to humid air with ~65% relative humidity during 4 days gives 100-150 nm thickness. The film is amorphous and has an oxidation rate less than 0.01 μm/y. The pH values between 8.5 and 11.5 correspond to a relatively protective oxide or hydroxide film; however above 11.5 a passive stable layer is observed. The poor corrosion resistance of many Mg alloys can be due to the internal galvanic corrosion caused by second phases or impurities. Agitation or any other means of destroying or preventing the formation of a protective film leads to increasing corrosion kinetics. The pH changes during pitting corrosion can come from two different reduction reactions: reduction of dissolved oxygen (O) and that of hydrogen (H) ions. Filiform corrosion was observed in the uncoated AZ31, while general corrosion mainly occurred in some deposition coated alloys. Crevice corrosion can probably be initiated due to the hydrolysis reaction. Exfoliation can be considered as a type of intergranular attack, and this is observed in unalloyed Mg above a critical chloride concentration.**

**Keywords** corrosion, magnesium, magnesium alloys

## 1. Introduction and Objectives

Magnesium (Mg), the world's lightest structural metal with a specific gravity of 1.74, occurs widespread in nature in the form of various compounds. The principal ores of Mg are dolomite, magnesite, and carnallite; Mg also exists in nature as the chloride in seawater, underground natural brines, and salt deposits. Seawater is a virtually unlimited source of Mg. It has been estimated that 6 million tons of Mg are present in each cubic mile of seawater and there are approximately 320 million cubic miles of seawater on earth (DOW Chemical, 1994).[1] For engineering applications, Mg is usually alloyed with one or more elements, which include aluminum (Al), manganese (Mn), rare earth (RE) metals, lithium, zinc (Zn), and zirconium (Zr).[1]

Mg is emerging as a light structural metal for current, new, and innovative applications. New alloys and composites are developed or being developed for present and new challenges. It is now almost admitted that corrosion of Mg is avoidable and can be controlled if we have the right alloy for the right application with an appropriate coating as recommended for certain applications. In fact, under normal environmental conditions, the corrosion resistance of Mg alloys is comparable or better than that of mild steel. Poor corrosion resistance is most of the time due to poor design, flux inclusions, surface contamination, galvanic couples, and incorrectly applied or inadequate surface protection schemes for specific applications. The objectives of this paper are to consider briefly the state of the art in a comprehensive approach of general and localized corrosion of Mg alloys. The emphasis of this review is given to localized corrosion; however, stress corrosion cracking, fatigue corrosion, and erosion-corrosion that may give or result from localized attack as pitting, for example, are not considered.

**Edward Ghali,** Department of Mining, Metallurgical and Materials Engineering, Laval University Quebec, Canada, G1K 7P4; and **Wolfgang Dietzel** and **Karl-Ulrich Kainer,** GKSS-Forschungszentrum GmbH, Institute for Materials Research, Center for Magnesium Technology, Geesthacht, Germany. Contact e-mail: edward.ghali@gmn.ulaval.ca.

## 2. Metallurgical Considerations

### *2.1 Some Current Magnesium Alloys*

**2.1.1 Magnesium-Aluminum Alloys.** The AZ alloys, which contain Zn as a secondary alloying element, solidify with a sufficiently fine grain size to meet most property requirements. They are highly castable and have a minimum tendency toward hot cracking; this tendency increases with increasing Zn content. These alloys also, however, have a tendency to develop microporosity. The alloy AZ91 is the most commonly used of all Mg alloys due to its relatively low cost and generally adequate mechanical properties and processing characteristics. AM60, which contains Mn as a secondary alloying element and has a typical elongation of 6% in the as-cast condition, was developed to provide higher ductility and toughness required for die cast automobile wheels. The second alloy, AS41, contains silicon (Si) and Mn as secondary alloying elements, being developed to provide improved elevated temperature properties for engine applications such as the crankcase of air-cooled engines.[2]

**2.1.2 Magnesium-Zinc-Alloys.** The extremely effective

precipitation hardening reactions of the Mg-Zn binary and the grain refining effect of zirconium (Zr) combine to yield high strengths with good ductility. The Mg-Zn alloys with Zr, thorium (Th), or RE elements can provide very good combinations of room temperature yield strength and elongation. As the zinc content in these alloys is increased, microporosity and hot cracking become a problem, and this tends to be less severe in the alloys containing Th or RE elements. All of these grades tend to be more costly than Mg-Al alloys.[2]

**2.1.3 Magnesium-Rare Earth, Thorium, and Silver Alloys.** These alloys, being relatively expensive, are used selectively when service temperatures exceed about 150 °C. Good elevated temperature properties are obtained through the development of stable grain boundary precipitates, and they generally have good castability. The Mg-RE alloys are susceptible to oxidation while the Mg-Th alloys have more severe oxidation problems.[2]

### *2.2 Alloying Elements and Newly Developed Alloys*

Al content in Mg alloys results in better castability and an increase of ambient tensile, compressive, and fatigue strength as well as improves the corrosion resistance. On the other hand, creep properties, and ductility and impact strength deteriorated significantly.[3] At low temperatures, Mg and Al alloys do not exhibit a ductile-brittle transition. The elastic modulus, and the notched and unnotched yield and tensile strengths remain constant or increase only slightly as the temperature decreases, and total elongation can increase or decrease slightly. At high temperatures, the commonly used Mg alloys are generally inferior to cast Al alloys in their behavior. AS41 was developed to improve upon the creep resistance of AZ91 although it still does not perform as well as die cast 380 Al, for example. The elastic modulus of Mg can also decrease significantly with increasing temperature; e.g., the modulus of the AZ alloys can decrease by approximately 15% at 150 °C and 30-50% at 250 °C.[2,3]

Poor creep resistance of current Mg alloys at temperatures above 125 °C make them inadequate for most powertrain applications in automobiles, transmission cases that operate at up to 175 °C, and engine blocks up to 200 °C.[4] When die cast AZ91 and AM alloys are subjected to elevated temperature creep conditions, the highly supersaturated α-Mg in the microstructure decomposes by discontinuous precipitation of $Mg_{17}Al_{12}$, resulting in the microstructure. There is reason to believe that this decomposition of the microstructure is the prime cause of the weakness of die cast AZ91 in creep. It is believed that the discontinuous precipitation reaction promotes grain boundary migration and sliding, which are prominent creep deformation mechanisms in Mg alloys. Generally the microstructures of die cast AE42 and AS21 contain very little of the highly supersaturated α-Mg and, as a result, very little microstructural decomposition occurs during elevated temperature exposure. These alloys also contain strong stable intergranular phases, which pin grain boundaries and further hinder both grain boundary migration and sliding.[4,5]

The intermetallic eutectic phase β-$Mg_{17}Al_{12}$ has an important role to play in imparting strength and stiffness to Mg-Al alloys, but the inherent brittleness of this phase limits the overall ductility unless it is controlled. One of the easiest ways of doing this is to reduce the volume fraction of β by lowering the Al content, as in alloys AM50 and AM60. Rare-earth additions to Mg are known to increase the resistance to creep deformation. Other elements with beneficial effect are Th, yttrium (Y), scandium (Sc), and silver (Ag). Most of the commercial Mg alloy systems that possess creep resistance are based on rare-earth or Y containing systems. These alloys, though widely used in aerospace applications, find limited use in the automotive industry due to the cost penalty.[5]

A new family of creep-resistant Mg alloys is based on the Mg-Al-Sr system. Creep resistance, the tensile yield strength, and the bolt-load-retention of these alloys at 150 °C and 175 °C show improvement over Mg-Al-RE and Mg-Al-Si system. The microstructure of the alloys is characterized by Al-Sr-(Mg) containing intermetallic second phases and the alloys exhibit better salt-spray corrosion resistance (0.09-0.15 mg/cm$^2$ day) than other commercial Mg die casting alloys such as AM60B, AS41, and AE42, and the Al die casting alloy A380.[6] The AJ alloys AJ52x and AJ62x have superior creep performance surpassing all other Mg alloys at high temperatures (150-175 °C) and high stresses (50-70 MPa). The most recent alloy formulation AJ62x (Mg-6Al-2Sr) has shown the highest tensile properties, excellent castability, and superior resistance to hot tearing and cracking. The ductility of the AJ62x version is an added advantage for this alloy. The alloys showed salt-spray corrosion resistance equal to or better than AZ91D.[7]

However, Aghion et al.[3] have pointed out that the price of Sr containing master alloys is considerably higher than that of other alloys such as calcium (Ca) containing master alloys and Ce-based mishmetal alloys. Also, the alloy AJ52X, for example, requires very specific casting conditions such as a casting temperature of 720 °C and die surface temperature of 300-350 °C, making it very difficult to die cast using the existing equipment.[3] Alloying with Ca provides the maximum increase of both ambient tensile and compressive yield strength, and especially creep strength for equal unit weight compared with strontium (Sr) and RE mishmetal. As Ca is a relatively inexpensive element, and has an atomic weight which is half that of strontium and less than one-third the atomic weight of RE elements, it is a very attractive alloying addition.[3] It is also evident that alloying with Ca in concentrations more than 0.3% causes castability and ductility deterioration. Hence, it is the challenge for alloy developers to select optimum combination of alloying ingredients (Al, Ca, Sr, RE) to provide mainly creep resistance and flow properties within an affordable cost regimen.[3]

A new creep resistance alloy development was demonstrated by Honda R&D Center[8] and General Motors R&D Center.[9] The alloy ACM522 developed by Honda is based on AM50 alloy with additions of 2.5% Ce-based mish metal and 2% Ca. This alloy is already in small-scale industrial use for production of oil pan for Honda's 1-L engine for the "Insight" hybrid car with fuel consumption of 35 km per liter. It was demonstrated that this alloy exhibits creep strength in the range of 150-200 °C, similar to that of Al alloy A384. However, ACM522 alloy, in addition to a rather high cost, has very low ductility (2-3%) and impact strength (4-5 J) that can limit its potential application. Furthermore, the presence of 2% Ca in this alloy can lead to hot cracking problems in components with variable wall thickness and more complicated shape than

specially designed oil pans with wall thicknesses in the range of 2.5-3 mm.[3,8,9]

The new AXJ alloy developed by General Motors R&D Center is based on AM50 alloy with addition of 1.7-3.3% Ca and up to 0.2% Sr. The alloy exhibits excellent creep resistance although its castability is very sensitive to Ca content.[9] The alloy named MEZ after Magnesium Electron[10] includes 2.5% RE, 0.35% Zn, and 0.3% Mn, with small additions of Zr or Ca. This alloy exhibits creep resistance and bolt load retention better than AE42 at temperatures within the range of 150-175 °C. However, MEZ alloy has very low ductility (1-2%) and low tensile yield strength (95-110 MPa) at room temperature.[3,9,10]

Mg and specialty Mg-lithium (Li) alloys, due to their superior stiffness-to-weight ratio, provide a promising matrix for composites in applications such as aerospace and aircraft structure as well as for structural components in ultra-lightweight communications systems. These alloys also show high electrical and thermal conductivities. However their poor resistance to corrosion and their low creep strength has slowed their development and industrial use. Recent work indicates that an important reinforcement of Mg-Li alloys is obtained with additions of SiC particulates or short fibers through the conventional melt route.[11] Li is a suitable alloying element, which apart from a density reduction, increases clearly the ductility of hexagonal Mg alloys as the comparisons with well-known Mg standard alloys have shown.[12] Solid solutions of Mg alloys with low Li contents (i.e., the so-called $\alpha$-phase alloys) retain the hexagonal structure and exhibit moderate strength albeit with low formability. The ductility is much improved with larger additions of Li, which bring about the formation of the centered cubic phase (i.e., the $\beta$ phase) but the strength is then notably lowered. High Li alloys containing the cubic phase exhibit lower creep properties. However, a two-phase structure ($\alpha+\beta$) constitutes an interesting compromise since it combines the moderate strength of the $\alpha$-phase with the excellent ductility of the $\beta$ phase. Also, superplastic behavior was reported recently for Mg-Li alloys with such a two-phase structure.[13] Al additions increase the tensile strength and hardness of Mg-Li alloys. Small additions of silicon in Mg alloys moderately increase the ductility. However, at high silicon concentrations, the brittle $Mg_{22}Si$ phase forms. Small additions of rare-earth elements such as cerium (Ce), lanthanum (La), praseodymium (Pr), yttrium (Y), and neodymium (Nd) usually provide an overall increase in the mechanical properties of Mg alloys due to solid-solution strengthening and fine dispersion of intermetallic phases. The tensile strength of the Mg-Li-Al-Si alloy was improved by rare-earth additions but at the expense of ductility.[14]

### 2.3 Processing and Properties

Mg alloy castings are produced by liquid and semi-solid molding processes: high and low pressure die casting, gravity casting, thixomolding, and squeeze casting, while wrought forming processes include extrusion, rolling of sheet and plate, and forging.[15] So far, Mg alloys are processed into components with over 95% manufactured by the high pressure die casting process (HPDC), particularly sand and permanent mold castings.[12,15]

The Mg-Al-Mn system constitutes the basis for all die casting alloys. The intrinsic ductility of Mg alloys generally decreases with increasing Al content, while the castability is improved. High injection speeds, high metal pressures, and the lack of efficient thermal barriers lead to extremely high cooling rates. This makes high-pressure diecasting unique, since the resulting refined microstructures provide excellent mechanical properties. Possible explanations of the improved castability may be the suppression of $Mg_{17}Al_{12}$, combined with the reduced content of casting defects like porosity. The $Al_{11}RE_3$ phase solidifies at temperatures near 600 °C, i.e., close to the temperature of initial solidification of the alloys with 6-8% Al. Additions of RE elements at a given Al content may improve ductility. If a challenging part is designed for AM50, an AE alloy with, for example, 6 wt.% Al can be used instead, giving the same mechanical properties. However, this alloy will offer the advantages of improved castability, and thus, an overall improvement in property performance. The corrosion properties will also be significantly improved.[16]

The Thixomolding process offers net shaping, improved mechanical properties, environmental cleanliness and decreased porosity.[17] Semi-solid metal casting was first developed at MIT in the 1970s and originally introduced as rheocasting or semi-solid metal processing (SSM). Thixomolding is the high-speed injection molding of semi-solid thixotropic alloys. The process consists of introducing Mg alloy feedstock in the form of metal granules at room temperature to a heated barrel and screw of a modified injection molding machine and then raising the temperature of the material to a semi-solid or liquid state under high shear rate mixing. The semi-solid slurry, consisting of nearly spherical solid particles suspended in a liquid matrix, is then injected into a preheated metal mold to make a net shape part. In contrast to die casting where the metal enters the die as turbulent streams of atomized sprays, the semi-solid thixotropic metal fills the mold generally in a planar flow front. This results in lower porosity than die castings and an ability to recycle scrap without secondary treatments.[18]

Unlike die casting, the process does not require separate melting and transfer systems for handling of molten metals. One potential disadvantage is the cost of granulate alloy feedstock relative to the alloy ingot used in the die casting process. Oxidation of granules should be avoided as far as possible. Properties for well made thixomolded products are generally similar to those of well made die castings, although claims are being made for lower porosity and thinner walls in thixomolded products.[15]

Ribbed sections, which can be thixomolded but not die cast, are being designed into new prototype runs to produce parts with significant weight savings while maintaining, or sometimes even increasing, strength. In areas where thermal management is critical, thinner wall sections, and even fins, can be molded without additional machining. This stands to greatly enhance the thermal dissipation in the final product. Net shape forming through thixomolding can reduce the cost of complex parts to the point where Mg components offer substantial improvements in thermal and electrical properties while eliminating machining and reducing finishing costs.[17]

New rheocasting (NRC) is a novel semi-solid casting process used to produce high quality castings. Originally designed

for Al alloy casting, laboratory trials on a 350 ton squeeze-casting machine gave promise for its introduction to the Mg casting market and was patented by UBE Industries Ltd. (Kirchdorf/Krems, Austria) (EP 07 45 694 Al).[20] The NRC process combines the common vertical squeeze casting approach with an integrated facility for producing globular material. A slurry maker carousel with various cooling stations and one induction heating station is also incorporated into the unit. Unlike conventional thixocasting or thixomolding, no special precursor material is needed. NRC allows Al castings to be produced for the automotive industry, which demands lightweight high-quality parts that have reproducible properties at an economic price.[19]

Here the semi-solid processing offers a way to produce thick-walled, pressure-tight, heat-treatable castings with little porosity and reduced susceptibility to heat cracks.[20] The essential point is that the NRC process uses conventional Mg alloys. The process is based on controlled cooling of a slightly superheated melt. This controlled cooling is performed in a carousel slurry maker. It is assumed that this process can support the use of Mg alloys in hydraulic components, engine mounts, or even suspension arms. While Thixomolding is used for thin-walled castings, NRC can be used for thicker walled parts, which must have limited porosity.[21]

**2.3.1 Skin Properties.** It has been shown that in certain situations about 20% of the material has been solidified into large (~20 μm) grains in a bimodal distribution form by dendritic solidification in the shot sleeve of the cold chamber die casting machine. Clearly the amount of such grains in die casting is dependent upon a number of casting parameters such as melt temperature, shot sleeve temperature, shot volume, and dwell time in the shot sleeve prior to application of the shot. Due to the very high rate of heat extraction, the surface layer (skin) of Mg die-castings has a very fine microstructure with very small (<0.5 μm) α-Mg grains and a higher volume fraction of the intergranular eutectic β-$Mg_{17}Al_{12}$ phase. This results in a hard surface layer, which can have a significant effect on the mechanical properties of the casting. Due to the higher volume fraction of β-$Mg_{17}Al_{12}$ in the surface layer, thin sections tend to have a slightly higher Young's modulus than thick sections, namely, 43.6 GPa for a 1mm thick casting compared with 42.3 GPa for 6mm thickness.[5]

### *2.4 Chemical Composition and Physical and Mechanical Properties of Some Commercial and Mentioned Alloys*

**2.4.1 Cast Alloys.** Two major cast Mg alloy systems are available to the designer. The first system includes alloys containing 2-10% Al, combined with minor additions of Zn and Mn. These alloys are widely available at moderate cost, and their mechanical properties are satisfactory from 95-120 °C (200-250 °F). At higher temperatures, the properties deteriorate. The second system consists of Mg alloyed with various elemental additions such as rare earths, Zn, Th, Ag, etc., except Al, and all contain a small but important Zr addition that imparts a fine grain structure, which improves mechanical properties. These alloys generally possess much better elevated-temperature properties, but their more costly elemental additions, combined with the specialized manufacturing technology required, result in significantly higher costs. Many of the casting alloys are given simple heat treatments to improve their properties, while the wrought alloys can be obtained in a number of tempers (see Table 1 for details).[14]

The insufficient creep strength of several commercial cast alloys is the original reason for the development of experimental Mg alloys. Low creep at relatively low elevated temperatures can cause poor bearing-housing contact, leading to oil leakage, increased noise and vibration, and/or more serious problems if used for various housings. It is also worthwhile to mention that one of the principal requirements of new Mg alloys is their cost point compared with existing Mg and Al alloys. This requirement combined with die castability issues reduces possible options to alloy systems containing Al or Zn as major alloying elements, with Mn, Si, Ca, Sr, and Ce-based mishmetal as relatively small additions. Table 2 summarizes the mechanical properties and corrosion performance of some experimental alloys as compared with commercial ones in Table 1.[3]

**2.4.2 Wrought Alloys.** Wrought materials are produced mainly by extrusion, rolling, and press forging at temperatures in the range of 300-500 °C. As with cast Mg alloys, the wrought alloys may be divided into two groups according to their Zr content (Table 3). Specific alloys have been developed that are suitable for wrought products, most of which fall into the same categories as the casting alloys. Examples of sheet and plate alloys are AZ31 (Mg-3Al-1Zn-0.3Mn), which is the most widely used one because it offers a good combination of strength, ductility, and corrosion resistance, and Th-containing alloys such as HM21 (Mg-2Th-0.6Mn), which show good creep resistance at temperatures of up to 350 °C. Mg alloys can be extruded at temperatures above 250 °C into either solid or hollow sections at speeds that depend upon alloy content. Higher strength alloys such as AZ81 (Mg-8Al-1Zn-0.7 Mn), ZK61 (Mg-6Zn-0.7Zr), and the more recent composition ZCM711 (Mg-6.5Zn-1.25Cu-0.75Mn), all have strength/weight ratios comparable to those of the strongest wrought Al alloys. The alloy ZM21 (Mg-2Zn-1Mn) can be extruded at high speeds and is the lowest cost Mg extrusion alloy available. Again, Th-containing alloys, such as HM31 (Mg-3Th-1Mn), show the optimal elevated temperature properties. Mg forgings are less common and are almost always press-formed rather than hammer-forged.

## 3. Active-Passive Behavior of Magnesium and Magneisum Alloys

### *3.1 The Potential-pH Diagram of Magnesium*

The Pourbaix (potential-ph) diagram[22] shows possible protection of Mg at high pH values, which may result from $Mg(OH)_2$ formation during the corrosion reaction. Perrault[23] considered the formation of $MgH_2$ and $Mg^+$ and assumed that thermodynamic equilibrium cannot exist for a Mg electrode in contact with aqueous solutions. Such equilibrium is, however, possible if the H overpotential is about 1 V and the pH is greater than 5. The following reactions are considered in the E-pH diagram[22,23] (Fig. 1):

**Table 1 Nominal Composition, Typical Tensile Properties, and Characteristics of Selected Magnesium Casting Alloys (Polmear, 1994)[14]**

| Designation | | Nominal Composition, wt.% | | | | | | | | | | | | Tensile Properties | | | |
|---|---|---|---|---|---|---|---|---|---|---|---|---|---|---|---|---|---|
| | | | | | | | | Rare Earth | | | | | | 0.2% Proof Stress | Tensile Strength | El | |
| ASTM | British | Al | Zn | Mn | Si | Cu | Zr | MM | Nd | Th | Y | Ag | Condition | MN m$^{-2}$ | MN m$^{-2}$ | % | Characteristics |
| AZ63 | | 6 | 3 | 0.3 | … | … | … | … | … | … | … | … | As sand cast | 75 | 180 | 4 | Good room temperature strength and ductility |
| | | … | … | … | … | … | … | … | … | … | … | … | T6 | 110 | 230 | 3 | |
| AZ81 | A8 | 8 | 0.5 | 0.3 | … | … | … | … | … | … | … | … | As sand cast | 80 | 140 | 3 | Tough, leak tight casting with 0.0015% Be used for pressure die casting |
| | | … | … | … | … | … | … | … | … | … | … | … | T4 | 80 | 220 | 5 | |
| AZ91 | AZ91 | 9.5 | 0.5 | 0.3 | … | … | … | … | … | … | … | … | As sand cast | 95 | 135 | 2 | General purpose alloy used for sand and die casting |
| | | … | … | … | … | … | … | … | … | … | … | … | T4 | 80 | 230 | 4 | |
| | | … | … | … | … | … | … | … | … | … | … | … | T6 | 120 | 200 | 3 | |
| | | … | … | … | … | … | … | … | … | … | … | … | As chill cast | 100 | 170 | 2 | |
| | | … | … | … | … | … | … | … | … | … | … | … | T4 | 80 | 215 | 5 | |
| | | … | … | … | … | … | … | … | … | … | … | … | T6 | 120 | 215 | 2 | |
| AM50 | | 5 | … | 0.3 | … | … | … | … | … | … | … | … | As die cast | 125 | 200 | 7 (a) | High pressure die castings |
| AM20 | | 2 | … | 0.5 | … | … | … | … | … | … | … | … | As die cast | 105 | 135 | 10 (a) | Good ductility and impact strength |
| AS41 | | 4 | … | 0.3 | 1 | … | … | … | … | … | … | … | As die cast | 135 | 225 | 4.5 (a) | Good creep properties up to 150 °C |
| AS21 | | 2 | … | 0.4 | 1 | … | … | … | … | … | … | … | As die cast | 110 | 170 | 4 (a) | Good creep properties up to 150 °C |
| ZK51 | Z5Z | … | 4.5 | … | … | … | 0.7 | … | … | … | … | … | T5 | 140 | 235 | 5 | Sand castings, good room temp. strength and ductility |
| ZK61 | | … | 6 | … | … | … | 0.7 | … | … | … | … | … | T5 | 175 | 275 | 5 | As for ZK51 |
| ZE41 | RZ5 | … | 4.2 | … | … | … | 0.7 | 1.3 | … | … | … | … | T5 | 135 | 180 | 2 | Sand castings, good room temp. strength and castability |
| ZC63 | ZC63 | … | 6 | 0.5 | … | 3 | … | … | … | … | … | … | T6 | 145 | 240 | 5 | Pressure tight castings, good elevated temp. Strength, weldable |
| EZ33 | ZRE1 | … | 2.7 | … | … | … | 0.7 | 3.2 | … | … | … | … | Sand cast | 95 | 140 | 3 | Good castability, presure tight, weldable, creep resistant up to 250 °C |
| | | … | … | … | … | … | … | … | … | … | … | … | T5 | 100 | 155 | 3 | |
| | | | | | | | | | | | | | Child cast T5 | | | | |
| HK31 | MTZ | … | … | … | … | … | 0.7 | … | … | 3.2 | … | … | Sand cast T6 T6 | 90 | 185 | 4 | Sand casting, good castability, weldable, creep resistant up to 350 °C |
| HZ32 | ZT1 | … | 2.2 | … | … | … | 0.7 | … | … | 3.2 | … | … | Sand or chill cast (T5) | 90 | 185 | 4 | As for HK31 |
| QE22 | MSR | … | … | … | … | … | 0.7 | … | 2.5 | … | … | 2.5 | Sand or chill cast (T6) | 185 | 240 | 2 | Pressure tight weldable high proof stress up to 250 °C |
| QH21 | QH21 | … | … | … | … | … | 0.7 | … | 1 | 1 | … | 2.5 | As sand cast | 185 | 240 | 2 | Pressure tight weldable, good creep resistance and proof stress up to 300 °C |
| | | … | … | … | … | … | … | … | … | … | … | … | T6 | | | | |
| WE54 | WE54 | … | … | … | … | … | 0.5 | … | 3.25(b) | … | 5.1 | … | T6 | 200 | 285 | 4 (a) | High strength at room and elevated temp, good corrosion resistance, weldable |
| WE43 | WE43 | … | … | … | … | … | 0.5 | … | 3.25(b) | … | 4 | … | T6 | 190 | 250 | 7 (a) | |

(a) Values quoted for tensile properties are for separately cast test bars and may not be realized in certain parts of castings
(b) Contains some heavy metal rare earth elements
MM mischmetal; El. elongation
Reproduced with permission from [14], Institute of Materials, London, U.K.

$$2H^+ + 2e \rightarrow H_2 \quad \text{(Eq 1)}$$

$$MgH_2 \rightarrow Mg^{2+} + H_2 + 2e^- \quad \text{(Eq 2)}$$

$$MgH_2 + 2\ OH^- \rightarrow Mg(OH)_2 + H_2 + 2e^- \quad \text{(Eq 3)}$$

$$Mg^{2+} + 2OH^- \rightarrow Mg(OH)_2 \quad \text{(Eq 4)}$$

$$Mg^+ \rightarrow Mg^{2+} + e^- \quad \text{(Eq 5)}$$

$$Mg^+ + 2OH^- \rightarrow Mg(OH)_2 + 1e^- \quad \text{(Eq 6)}$$

$$Mg^+ + 2\ H_2O \rightarrow Mg(OH)_2 + 2\ H^+ + e^-$$

$$MgH_2 \rightarrow Mg^+ + H_2 + e^- \quad \text{(Eq 7)}$$

**Table 2 Ultimate Tensile Strength, Elongation, and Corrosion Rate of Some Experimental and Commercial Cast Magnesium Alloys**

| Designation ASTM | Major Alloying Elements | UTS, MPa | | Elongation, % | | Corrosion Rate, (mg/cm$^2$/day) (a) | Reference Number |
|---|---|---|---|---|---|---|---|
| | | 20 °C | 150 °C | 20 °C | 150 °C | | |
| AZ91D | Commercial (Al, Zn) | 260 | 160 | 6 | 18 | 0.11 | 3 |
| AE42 | Commercial (Al, RE | 240 | 160 | 12 | 22 | 0.12 | 3 |
| AS21 | Commercial (Al, Si) | 230 | 120 | 16 | 27 | 0.34 | 3 |
| MRI 153M | Experimental Al, Ca, Sr, RE (Be Free) | 250 | 190 | 6 | 17 | 0.09 | 3 |
| MRI 230D | Experimental (Al, Ca, Sr, RE) | 235 | 205 | 5 | 16 | 0.10 | 3 |
| AJ62Lx | Experimental (5.6–6.4% Al, 1.7–2.21% Sr) | 276 | | 12 | | 0.04 | 6 |
| AJ62x | Experimental (5.6–6.4% Al, 1.7–2.21% Sr) | 240 | | 7 | | 0.11 | 6 |
| AE | Experimental (5–9% RE) | 280 | | 10–12 | | 0.02–0.04 (b) | 16 |
| AM60 | Commercial (6% Al, 0.13% Mn) | | | | | 0.055 (b) | 16 |
| AXJ | Experimental (0.87–2.6% Ca, up to 0.17% Sr) (c) | | (d) | | (d) | approx. 0.11 | 9, 48 |

(a) 200 h Salt Spray Test (ASTM Standard B-117)
(b) 10 days Salt Spray Test (ASTM Standard B-117)
(c) Optimum overall castability at 2% Ca
(d) 20% greater creep strength than AE42 at 150 °C

### *3.2 General Corrosion*

The corrosion potential of Mg is slightly more negative than −1.5 V in dilute chloride solution or a neutral solution with respect to the standard H electrode due to the polarization of the formed Mg $(OH)_2$ film since Mg standard electrode potential at 25 °C is −2.37 V. This indicates that the metal corrodes with an accompanying fairly stable film of rather low conductivity even in acidic solutions. The oxide film on Mg offers considerable surface protection in rural and some industrial environments, and the corrosion rate of Mg lies between that of Al and that of low carbon steels (Table 4).[24] Passivity of Mg is destroyed by several anions, including chloride, sulfate, and nitrate. Chlorides, even in small amounts, usually break down the protective film on Mg. Fluorides form insoluble Mg fluoride and consequently tend to passivate. The presence of oxidants, such as chromate, vanadates, phosphates, and others that promote the formation of a protective layer, tend to retard corrosion.[25]

In natural atmospheres, the corrosion of Mg can be localized. The conductivity, ionic species, temperature of the electrolyte, alloy composition and homogeneity, differential aeration, etc. influence the corrosion morphology.

Effective corrosion prevention for Mg components and assemblies begins at the design stage. General corrosion attack in salt-water exposures can be minimized through the selection of high-purity Mg alloys cast without introducing heavy metal contaminants and flux inclusions.

**3.2.1 Formation and Properties of the Barrier Film.** Mg exposed to air is covered by a gray oxide film, which can offer considerable protection to Mg exposed to atmospheric corrosion in rural, most industrial and marine environments. In aqueous media, Mg may form a surface film, which protects it in alkaline environments, and poorly buffered environments. This may result from $Mg(OH)_2$ formation during the corrosion reaction and can increase the pH. In aqueous solutions, Mg dissociates by electrochemical reaction with water to produce a crystalline film of Mg hydroxide and hydrogen (H) gas, a mechanism, which is highly insensitive to the oxygen (O) concentration, generally in absence of oxidizing agents. Then, sites of H discharge can control the corrosion rate according to the total reaction:

$$Mg(s) + 2H_2O(\ell) \rightarrow Mg(OH)_2(s) + H_2(g)$$

The oxide layer is composed of $(MgO \cdot H_2O)$. The film formed in air immediately after scratching the metal surface is initially thin, dense, amorphous, and relatively dehydrated. The oxide thickness on pure Mg after exposure for only ~10 s at ambient is 2.2 ± 0.3 nm (approximately seven mono-layers of MgO) and increases slowly, linearly with the logarithm of exposure time during a test of 10 months period.[26] Continuing exposure to humid air or to water leads to the formation of a thicker hydrated film adjacent to the metal. Exposure to ambient air for a period of 15-60 min gives a film thickness of 20-50 nm, while exposure to humid air with ~65% relative humidity during 4 days gives 100-150 nm thickness.[27] In the case of Al, the air-formed oxide film on the surface is an amorphous Al oxide, 2-4 nm thick at room temperature and this oxide appears to reach a terminal thickness after 1 h exposure. [26]

The morphology and structure of oxide films on Mg, formed by immersion in distilled water after 48 h, have been shown to be composed of a three-layer structure, consisting of an inner cellular structure (0.4-0.6 μm), a dense intermediate region (20-40 nm) and an outer layer with a platelet like morphology, around 2 μm in thickness (Fig. 2). The hydrated inner and the intermediate layers are similar in structure to the air-formed film.[24]

The Mg oxide should be hydrated to produce hydrated Mg oxide as the Al oxide does. The hydroxide film, brucite, has a hexagonal crystalline structure, which is layered, alternating between Mg and hydroxide ions, facilitating easy basal cleavage. Cracking and curling of the film have been noted though it is not clear whether it is from the properties of the film or the evolution of H gas. The Pilling-Bedworth ratio for $Mg(OH)_2$ is 1.77, which indicates a resistant film in compression. A combination of internal stresses and easy basal cleavage may account for a portion of the cracking and curling of the film. Thus, the structure of the corrosion product directly influences the corrosion behavior of the base metal.[28]

**Table 3 Nominal Composition, Typical Tensile Properties, and Characteristics of Selected Wrought Magnesium Alloys (Polmear, 1994)[14]**

| Designation | | Nominal Composition, wt.% | | | | | | | | Tensile Properties | | | |
|---|---|---|---|---|---|---|---|---|---|---|---|---|---|
| ASTM | British | Al | Zn | Mn | Zr | Th | Cu | Li | Condition | 0.2% Proof Stress MN $m^{-2}$ | Tensile Strength MN $m^{-2}$ | El., % | Characteristics |
| Ml | AM503 | … | … | 1.5 | … | … | … | … | Sheet, plate/F | 70 | 200 | 4 | Low to medium strength |
| | | | | | | | | | Extrusions/F | 130 | 230 | 4 | alloy, weldable, |
| | | | | | | | | | Forgings/F | 105 | 200 | 4 | corrosion resistant |
| AZ31 | AZ31 | 3 | 1 | 0.3 | … | … | … | … | Sheet, plate/O | 120 | 240 | 11 | Medium strength alloy, |
| | | | | 0.2(a) | | | | | Sheet, plate/H24 | 160 | 250 | 6 | weldable, good |
| | | | | | | | | | Extrusions/F | 130 | 230 | 4 | formability |
| | | | | | | | | | Forgings/F | 105 | 200 | 4 | |
| AZ61 | AZM | 6.5 | 1 | 0.3 | … | … | … | … | Extrusions/F | 180 | 260 | 7 | High strength alloy, |
| | | | | 0.15(a) | | | | | Forgings/F | 160 | 275 | 7 | weldable |
| AZ80 | AZ80 | 8.5 | 0.5 | 0.2 | … | … | … | … | Forgings/T6 | 200 | 290 | 6 | High strength alloy |
| | | | | 0.12(a) | | | | | | | | | |
| ZM21 | ZM21 | … | 2 | 1 | … | … | … | … | Sheet, plate/O | 120 | 240 | 11 | Medium strength alloy, |
| | | | | | | | | | Sheet, plate/H24 | 165 | 250 | 6 | good formability, good |
| | | | | | | | | | Extrusions/F | 155 | 235 | 8 | damping capacity |
| | | | | | | | | | Forgings/F | 125 | 200 | 9 | |
| ZMC71 1 | | … | 6.5 | 0.75 | … | … | 1.25 | … | Extrusions/T6 | 300 | 325 | 3 | High strength alloy |
| LA141 | | 1.2 | … | 0.15(a) | … | … | … | 14 | Sheet, plate/T7 | 95 | 115 | 10 | Ultralight weight (specific gravity 1.35) |
| ZK31 | ZW3 | … | 3 | … | 0.6 | … | … | … | Extrusions/T5 | 210 | 295 | 8 | High strength alloy, |
| | | | | | | | | | Forgings/T5 | 205 | 290 | 7 | some weldability |
| ZK61 | | … | 6 | … | 0.8 | … | … | … | Extrusions/F | 210 | 285 | 6 | High strength alloy |
| | | | | | | | | | Extrusions/T5 | 240 | 305 | 4 | |
| | | | | | | | | | Forgings/T5 | 160 | 275 | 7 | |
| HK31 | | … | … | … | 0.7 | 3.2 | … | … | Sheet, plate/H24 | 170 | 230 | 4 | High creep resistance up |
| | | | | | | | | | Extrusions/T5 | 180 | 255 | 4 | to 350 °C, weldable |
| HM21 | | … | … | 0.8 | … | 2 | … | … | Sheet, plate/T8 | 135 | 215 | 6 | High creep resistance up |
| | | | | | | | | | Sheet, plate/T81 | 180 | 255 | 4 | to 350 °C, short time |
| | | | | | | | | | Forgings/T5 | 175 | 225 | 3 | exposure up to 425 °C, weldable |
| HZ11 | ZTY | … | 0.6 | … | 0.6 | 0.8 | … | … | Extrusions/F | 120 | 215 | 7 | Creep resistance up to |
| | | | | | | | | | Forgings/F | 130 | 230 | 6 | 350 °C, weldable |

(a) Minimum
Reproduced with permission from [14], Institute of Materials, London, U.K.

**3.2.2 Solution pH.** The Pourbaix potential-pH diagram shows possible protection of Mg at high pH values starting at 8.5 when the activity of Mg ions is equal to 1 M at 25 °C under atmospheric pressure while Al oxide film is stable in the pH range of 4.0-9.0.[22,23] The relatively high pH of Mg hydroxide (10.4) allows Mg to resist well strong bases. At acidic and neutral pH, the barrier layer on Mg is difficult to detect; however, at pH 9 a thick white precipitate of Mg hydroxide begins to form on the outside of the inner film. The pH values between 8.5 and 11.5 correspond to a relatively protective oxide or hydroxide film. However, above 11.5, a passive Mg hydroxide layer dominates the electrochemical behavior of Mg.[25]

**3.2.3 Passive Properties and Stability.** The quasi-passive hydroxide film on Mg is much less stable than the passive films formed on Al or stainless steels, for example.[29,30] Generally, the corrosion rate of Mg alloys lies between that of Al and that of mild steel. Amorphous oxides are in general regarded to have better passive properties than the crystalline ones. Al oxide is a stable amorphous one while Mg oxide is more prone to crystallization in the form of MgO, as a result of dehydration.[31] There are two main processes of attack of the passive Mg surface: conversion of the protective surface film to soluble bicarbonates, sulfites and sulfates which are washed away by rain and/or stimulation of local cell action by chloride ions.[32]

The film is amorphous and has an oxidation rate less than 0.01 μm/y. In general, the Mg corrosion products resulting from the anodic reaction depend on the environment and may include carbonate, hydroxide, sulfite and/or sulfate compounds. C dioxide and sulfur dioxide play an important role in the stability and composition of the film. A mixture of crystalline hydroxycarbonates of Mg hydromagnesite, $Mg\ CO_3 \cdot Mg\ (OH)_2 \cdot 9H_2O$, nesquehonite $MgCO_3 \cdot 3H_2O$, and lansfordite $MgCO_3 \cdot 5H_2O$ are reported to be an oxidation product on Mg; hydromagnesite and hydrotalcite $Mg_6\ Al_2\ (OH)_{16}\ CO_3 \cdot 4H_2O$ are formed on AZ 31 B. In an industrial atmosphere with high $SO_2$ content, traces of $MgSO_4 \cdot 6H_2O$ and $MgSO_3 \cdot 6H_2O$ were detected in addition to the hydroxy-carbonate products for an unalloyed ingot.[33]

### *3.2.4 Influence of Oxygen and Some Active Ions*

The influence of O concentration in aqueous media is not completely agreed on. Dissolved O plays no major role in the

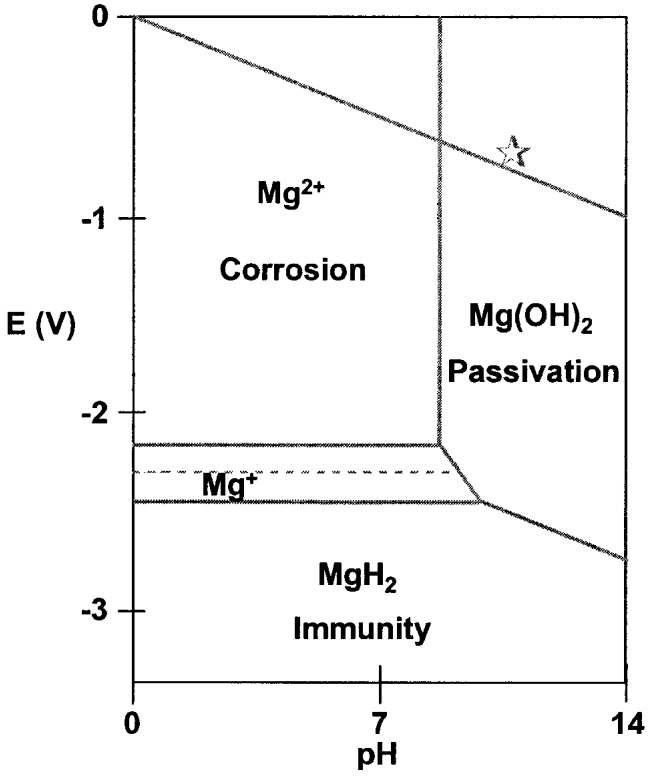


**Fig. 1** Equilibria of Mg-$H_2O$ system in presence of $H_2$ at 25 °C[22]

**Table 4 Results of 2.5 Year Exposure Tests on Sheet Alloys[24]**

| Material | Corrosion Rate, (μm/year) | Tensile Strength Loss (after 2-5 years, %) |
|---|---|---|
| Marine atmosphere | | |
| Al alloy 2024 | 2.0 | 2.5 |
| Mg alloy AZ31 | 18.0 | 7.4 |
| Low C steel (0.27% C) | 150.0 | 75.4 |
| Industrial atmosphere | | |
| Al alloy 2024 | 2.0 | 1.5 |
| Mg alloy AZ31 | 27.7 | 11.2 |
| Low C steel (0.27% C) | 25.4 | 11.9 |
| Rural atmosphere | | |
| Al alloy 2024 | 0.1 | 0.4 |
| Mg alloy AZ31 | 13.0 | 5.9 |
| Low C steel (0.27% C) | 15.0 | 7.5 |

corrosion of Mg in either fresh water or saline solutions.[24] Mg dissolution in aqueous environments generally proceeds by an electrochemical reaction with water to produce Mg hydroxide and H gas, so that Mg corrosion is relatively insensitive to the oxygen concentration. Some schools perform experiments without de-aeration or stirring to simulate practical conditions, and it has been mentioned that the percentage of O does not influence corrosion rates at least in certain circumstances.[34]

However, the presence of O is an important factor in atmospheric corrosion.[35] The most positive potentials are observed in pure water and alkaline solutions containing sub-critical amounts of certain anions. These potentials are usually near the

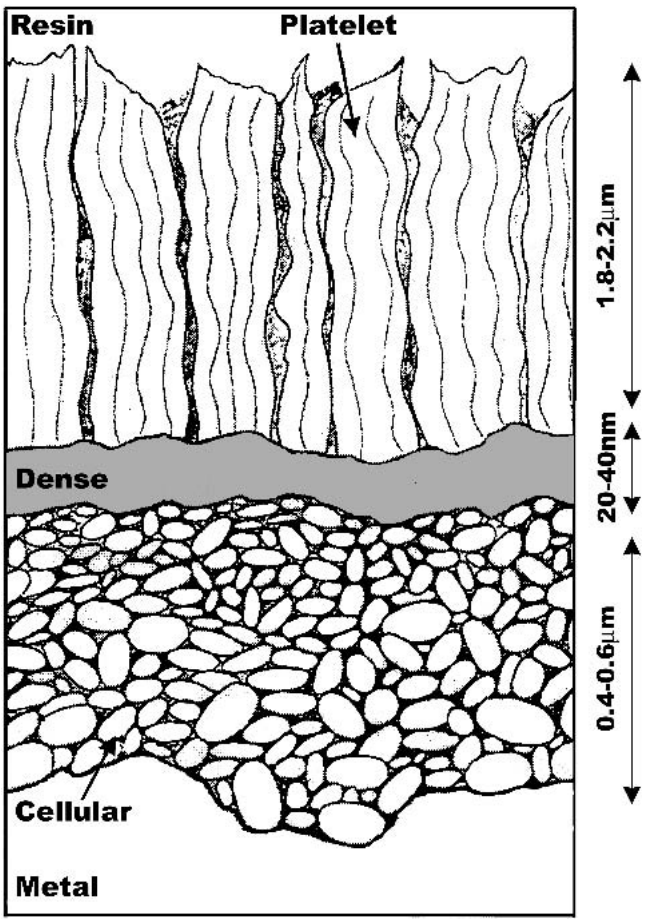


**Fig. 2** Schematic presentation of the three layer structure of the oxide films on Mg[27]

H electrode reversible potential, or readily raised thereto, by application of a very small anodic current. Only in environments of this type, and then under good aeration, does oxygen reduction play a significant role.[32] As the potential is lowered due to the presence of anions, O reduction becomes negligible relative to H evolution.[32,35]

The solubility of air and O in saline solutions decreases with increasing concentration of the salt, but salt increases the solution conductivity. The two effects combine in O reduction cathodic systems to produce increasing corrosion rates up to about 3.5 wt.% sodium (Na) chloride solutions and decreasing corrosion rates above that.[36] It has been shown that O plays a major role in the initiation of pitting of AZ 91, HK31 and some Mg-Zn alloys in 5 wt.% Na chloride solution at room temperature at relatively high corrosion potentials. This concern of initiation of pitting by the O reduction reaction can be extrapolated to other forms of localized corrosion. In acidic solution, and at more negative potentials, it seems that H reduction is the main cathodic reaction.[37] Hanawalt et al.[38] stated that the H overvoltage on pure Mg is high and is greatly lowered by iron (Fe), with no correlation of corrosion effect with H overvoltage.[38]

The ability of an anion to reduce the Mg potential appears to depend on the solubility of its Mg salt. It has been suggested

that anions are carried by electrochemical transport to anodic sites on the metal surface, where they form Mg salts, which are acidic to the Mg hydroxide film. The rapid uniform corrosion rate observed in 3M $MgCl_2$ at a lower electrode potential supports this mechanism.[39] Examples of these activating anions are $Cl^-$, $Br^-$, $SO_2^{-2}$, and $ClO_4^-$. In the presence of salt solutions of these anions, Mg becomes several tenths of a volt active with respect to the H electrode potential. H discharge becomes the controlling factor on effective sites as elements of low H overvoltage other than that of the hydroxide film itself due to its poor electronic conduction.[32] Baril and Pebere[40] studied the corrosion behavior of pure Mg in aerated and de-aerated solutions (0.01 and 0.1 M) by steady-state current-voltage and electrochemical impedance measurements. It was shown that the anodic current densities were lower and the resistance values higher in de-aerated media. They have stated that the presence of O does not influence the cathodic reaction and so O has no effect on Mg corrosion; however the shift of the potential in the cathodic direction in aerated solutions and higher anodic corrosion current densities can be explained by the presence of bicarbonate ion in natural conditions (40 mg $HCO_3^-$/l). Around the corrosion potential, on the anodic side, the current was dependent on the rotation rate, so the process should be partially controlled by diffusion.[40] They showed that the corrosion rate is dependent on $HCO_3^-$ concentration and as a consequence of the presence of $CO_2$ in solution. The impedance measurements showed that the corrosion rate of Mg rapidly reached a plateau during immersion in sodium sulfate, and a porous layer on the Mg surface is formed. They stated that the $HCO_3^-$ increased the rate of dissolution by the formation of soluble salts.

### 3.3 Agitation Influence

Agitation or any other means of destroying or preventing the formation of a protective film leads to corrosion. When Mg is immersed in a small volume of stagnant water, its corrosion rate is negligible. When the water is completely replenished, the solubility limit of Mg $(OH)_2$ is never reached, and the corrosion rate increases. In stagnant distilled water at room temperature, Mg alloys rapidly form a protective film that prevents further corrosion. Small amounts of dissolved salts in water, particularly chlorides or heavy metal salts will break the protective film locally, which usually lead to pitting.[24]

### 3.4 Temperature Influence in Aqueous Media

Pure Mg (99.5+ % purity < 10 ppm: Fe + Ni + Cu) immersed in distilled water, from which acid atmospheric gases have been excluded, is also highly protected. However, this good resistance to corrosion in water at room temperature decreases with increasing temperature, corrosion becoming particularly severe above 100 °C. The corrosion of Mg alloys by pure water increases substantially with temperature. At 100 °C, the AZ-alloys corrode typically at 0.25-0.50 mm/y. Pure Mg and alloy ZK 60 A corrode excessively at 100 °C with rates up to 25 mm/y. At 150 °C, all alloys corrode excessively. Another example, the alloy (AZ 31 B) has a corrosion rate of 0.43 mm/y (17 mpy) at 100 °C, but 30.5 mm/y at 150 °C.[32] Water vapor in air or in O sharply increases the rates of oxidation of Mg and its alloys above 100 °C, but boron trifluoride ($BF_3$), $SO_2$, and $BF_6$ are effective in reducing the oxidation rates.[24]

The increase in corrosion rate, with increasing temperature in ternary alloys is higher than that of pure Mg and may be due to the activation of some impurities in the ternary alloy at higher temperatures. It appears that the onset of pitting in a given alloy and in certain media depends on a critical pitting temperature below which only uniform corrosion is encountered. The corrosion of AZ 31 in Mg perchlorate with temperature revealed only a gradual increase without pitting.[29,30] Increasing temperatures sometimes precipitates protective salts, such as Ca carbonate, which decreases corrosion rates in normal-to-hard waters. Temperature differentials between points in a flow system can produce accelerated attack due to differences in ionic activity. The hot zones are generally anodic in the start; however, protective scales occasionally precipitate on the high-temperature metal surface regions and attack proceeds at the cooler sites.[36] Carbonate scaling and its measurement through the Langelier Index should be determined. Temperature increase generally decreases solubility of gases in open aqueous solutions, particularly O. This reduces the cathodic action, or more exactly that portion due to O reduction that is not determined precisely till now for Mg and Mg alloys and so the decrease of the amount of anodic reaction is not guaranteed.[29,30,36]

### 3.5 Atmospheric Oxidation

At room temperature, there is a significant difference in corrosion resistance between alloy constituents, and in a NaCl aqueous environment, the $Mg_{17}Al_{12}$ phase exhibits a better resistance by nearly one order of magnitude than $\alpha$-Mg.[41] Although the majority of present applications of Mg alloys cover room temperature environments, the alloys are subjected to high temperatures and detrimental contact with an oxidizing medium at various stages of manufacture including heat treatment, welding, casting, various routes of semisolid processing or future automobile applications, for example. A requirement of the removal of the skin layer, degraded by reheating prior to thixocasting and thixoforming, not only causes losses of material, but also contributes to a reduction in the billet temperature, important for the further stage of die-cavity filling.[41]

In Fig. 3, it is seen that the commercial AZ91D Mg alloy, tested at a temperature of 197 °C, does not increase its mass for time periods as long as 10 h. The measurements conducted at 437 °C revealed an accelerated mass gain after approximately 30 min of the reaction and this indicates that the capacity of protection of the oxide barrier disappears progressively in a critical temperature zone. The diffusivity (D) of Mg within the MgO lattice at 400 °C is as low as $2.24 \times 10^{-18}$ $m^2/s$, justifying negligible mass gains. Due to the large difference in densities between the oxide and metal, expressed by the MgO to Mg volume ratio of 0.81, the scale should not form a compact layer. Observations show, however, that no systematic spallation of oxide occurs in the thin film range where it exhibits highly protective behavior. The inherent strength of the thin MgO film in which the stress is operating is essentially two-dimensional, and the oxide can withstand the tensile stress necessary to adapt to the dimensions of the metal. Rupturing occurs only after the film exceeds a critical thickness as a

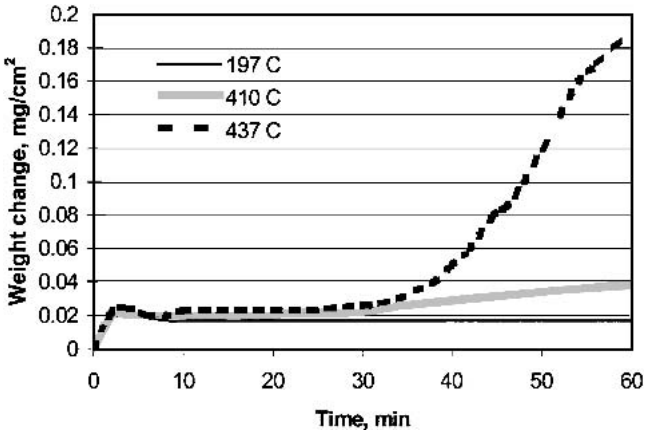


**Fig. 3** Exemplary atmospheric oxidation kinetics of an AZ91D alloy in air[41]

function of longer times and higher temperatures. Accelerated, non-protective oxidation is expressed by the growth and coalescence of oxide nodules, subsequently transformed to scales with a loose structure.[41]

## 4. Corrosion Influenced by Metallurgical Properties

### *4.1 Intergranular Corrosion*

Intergranular corrosion (IGC) of Mg alloys does not occur because the grain-boundary constituent is invariably cathodic to the grain body. Corrosion of Mg alloys is concentrated in the grains, and the grain-boundary constituent is not only more resistant to attack, but is cathodically protected by the neighboring grain.[28,42] However, in the early stages of immersion, a localized attack of Mg and its alloys can be formed at the grain boundary at the interface of cathodic precipitates in mild corrosive media and can be considered as intergranular (intercrystalline) corrosion. Since IGC has much sharper tips than pitting corrosion, it is a more drastic stress riser and has a more damaging contribution to corrosion fatigue.

Figure 4 shows the corroded surface of alloy AE81 after the hydroxide film has been stripped off in chromic acid. The grain bodies with a low Al concentration corrode at a faster rate than the Al-rich regions along the grain boundaries, as can also be seen in other Mg-Al alloys. However, in AE alloys, the pits do not easily penetrate the Al-rich zones. Good pitting resistance of the die-cast AE alloys is, therefore, attributed to the presence of these Al-rich zones, which appear to act as barriers against pit propagation. If these barriers are removed by a homogenization heat treatment, the corrosion resistance is reduced. Homogenized AE81 exhibited corrosion rates more than 100 times higher than the as-cast material during a three-day immersion test in 5% NaCl solution. It is not yet clear whether this unusual sensitivity of corrosion to heat treatment is related to the absence of Mn in this AE81 alloy. The corrosion rate of alloys AM80 and AZ91 were only moderately influenced by a similar heat treatment. In general, homogenized specimens exhibited deeper localized attack than the as-cast material.[24,28]

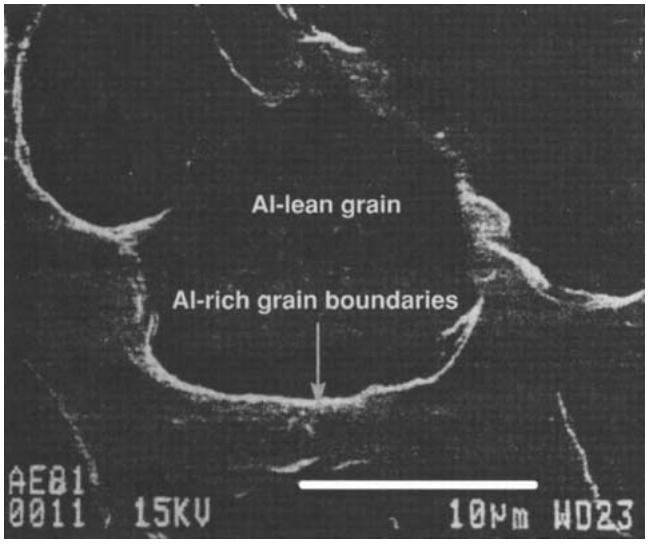


**Fig. 4** Morphology of corroded AE81 after removal of the hydroxide film[42]

**4.1.1 Exfoliation Corrosion.** Exfoliation can be considered as a type of intergranular attack, and this is observed in unalloyed Mg above a critical chloride concentration. This morphology was not seen in Mg alloys, in which individual grains were preferentially attacked along certain crystallographic planes. The early stages of this form of attack caused swelling at points on the surface due to apparent delamination of the Mg crystals with interspersed corrosion products, but as attack proceeded, whole grains or parts of grains disintegrated and dropped out, leaving the equivalent of large irregularly shaped pits.[43]

### *4.2 Alloying Elements and Corrosion*

Concentrations above 4% of Al in Mg alloys have been reported to give a significant increase of corrosion resistance to them. Influence of Al on MgO passive film has been examined by Nordlein.[31] Beldjoudi et al.[45] synthesized Mg-9Al, Mg-3Al, $Mg_{17}Al_{12}$, and AZ91E from high purity materials and studied their corrosion behavior in a 5% NaCl solution saturated with $Mg(OH)_2$. Corrosion rates were determined for each material including pure Mg using polarization resistance methods after about 80 min of exposure. Except for Mg, corrosion rates were remarkably similar with the $Mg_{17}Al_{12\ material}$ (i.e., lowest at 9$\mu$A/cm$^2$).[44,45] Danielson and Jones[46] showed that the corrosion rates determined by polarization resistance in aerated 3.5% NaCl solution after 48 h of exposure are as follows: AE42 > ZAC8506 > AZ91D. This general trend follows the Al content with the highest Al concentration resulting in the lowest corrosion rate. The inner surface of the ZAC8506 corroded at a rate almost a factor of six greater than the mold-side surface. The spherical particles in the thixomolded alloys appear to be more resistant to corrosive attack even when the particles showed some signs of aging compared with the surrounding matrix, probably due to the high Al content in solid solution.[46]

The alloys ZM5-A and ZM-6, which were prepared using

the pure Mg ingots produced by the Pidgeon process, i.e., distilled Mg, showed better corrosion resistance than ZM5-B and ZM6-B, which were prepared using pure Mg ingots produced by electrolytic process. For the same purity grade, the distilled Mg may possess less of the impurity elements Fe, Ni, Cu, and Cl than electrolytic Mg.[47] Impurities, such as Fe, Ni, Cu, Cl, etc., could accelerate the corrosion of these Mg alloys, especially for ZM5, while alloying elements Zr and/or Nd could increase corrosion resistance of ZM1 and ZM6.[47] It has also been shown that melting Mg carefully and alloying with Zr and other RE elements such as Nd improve the corrosion resistance of Mg alloys.[47]

Other work by Pettersen et al.[8] has been done to improve the corrosion resistance of AS21 by exchanging Mn with RE elements, based on the mutually limited solubility of Mn and RE in the AS-based alloys. AS21X alloys with RE in the range 0-0.4 wt.% and Mn in the range of 0-0.35 wt.% were produced in 100 kg batches in mild steel crucibles. Standard protection gases were used. The alloys were produced at 740 °C, and thereafter stabilized stepwise at 720, 700, 680, and 660 °C. At each of these temperatures both permanent mold-cast disk samples and die-cast test plates were produced. The Fe content was below 40 ppm in all specimens cast at 720 °C and below. The die cast test plates were corrosion tested in salt spray for 240 h according to ASTM B117. The correlation between Mn-content and corrosion rate is clear, showing an optimum for 0.05-0.1 wt.% Mn, and a corresponding RE content of around 0.15 wt.%. The study of the intermetallic particles in the die cast material shows a significant difference in particle compositions between AS21 and AS21X, which can explain the improved corrosion behavior of AS21X.[8]

The overall effect of an alloying element on corrosion rate depends on where and in what form and amount it is present in the alloy. Since both AC52 and AC53 were prepared by adding Ca to AM50, the addition of Ca first decreases the corrosion rate and then increases it. Calcium initially dissolves in Mg and improves its corrosion properties by lowering its activity. On further increasing the concentration of Ca in Mg, Ca forms an intermetallic compound $(Mg_2Al)_2Ca$ with Al and Mg,[48] which is probably more cathodic in nature than Mg, and therefore, increases the corrosion rate. Additions of 0.3% Si in AC53 increase the corrosion rate of the alloy, but the rate decreases upon adding Sr to AC53 + 0.3%Si. Both Ca and Sr are anodic to Mg, and therefore, both elements in small amounts reduce the corrosion of Mg. On the other hand, Si increases corrosion because it is cathodic to Mg.[49]

### 4.3 Influence of Alloying Elements and Microstructure on Passivation

Alloying affects the nature of the barrier film, but these effects are poorly understood. The presence of the elements Fe, Mn, Al, Ca, and Sr as a part of the corrosion products and their influence on the protection quality of the Mg oxide film has not been completely examined. Another important consideration is that modification of the oxide properties of Mg alloys can lead to further improvements in corrosion resistance of Mg alloys.[44] The corrosion of Mg and its alloys is also strongly dependent on the absence of impurity elements, some of which have well-defined tolerance levels above which corrosion resistance drops dramatically. For conventional Mg alloys, these tolerance limits must be observed even if extensive surface treatments are applied. These elements may influence the composition, adhesion, and protective quality of the hydroxide film.

Atmospheric conditions give thicknesses of between 1 and 15 nm on pure and several Mg alloys.[26] In the case of pure Mg with Al (3-8.5 wt.%), an initial oxide film is formed, which is thicker than that formed on Al or Mg metals. However, it should be noted that after this initial attack, the oxidation rates are all significantly lower than for pure Mg during the first week of exposure. It is believed that the presence of Al ions in the oxide film increases the activation energy for ion movement.[26,50] With increasing Al content of the alloy, all layers become dehydrated and enriched in Al oxide. Furthermore, the innermost and outermost layers decrease in thickness. These changes are particularly significant when the Al content of the alloy is increased above 4%, which corresponds to about 35% Al in the innermost layer. This threshold is characterized by a significant improvement in the corrosion resistance. It has been shown that Zn is the fastest diffusing of the components in the Mg–Al–Zn ternary system. Zn could thus compete with Al for sites in the MgO lattice and would then lessen the beneficial effects of the former ion. Mg containing low concentrations of impurities of Fe or Mn is shown to oxidize significantly more rapidly than pure Mg does. The impurities are present as inclusions, and localized oxidation is enhanced in their vicinity around the Mn and Fe inclusions.[26]

The β phase is inert to the chloride solution in comparison to the Mg matrix and acts as a corrosion barrier depending on the manner in which the $Mg_{17}Al_{12}$ phase is distributed (Fig. 5). The corrosion resistance of the β phase, observed generally in the cast alloy, can be related to its passive behavior within a much wider pH range than its pure components.[51,52] Mathieu et al.[34] showed that galvanic corrosion occurs in AZ91D die-cast and semi-solid castings between the two main phases, α and β. However, it has been stated that the semi-solid process induces strong modification of the microstructure of AZ91D alloy in terms of distribution, composition, and volume fraction of the constituent phases, and these castings have shown a corrosion rate at least 35% below that of the die-cast alloy. The better corrosion behavior of thixocast alloys is, thus, attributed to the particular composition of the α-phase resulting from the treatment of the α-phase (3 wt.% Al versus 1.8 wt.% Al for die-cast alloy). Semi-solid castings lead to structures with large rounded grains in a solid solution of Mg (α phase $Mg_4Al$) whereas the die-cast alloys are more homogeneous. Also, the whole surface area of the β cathodic phase is very low compared with that of the α-phase, and the β phase contains more Zn in the thixocast alloy.[34] Daloz et al.[53] have shown that Zn increases the potential and decreases the corrosion current rate of the β phase ($Mg_{17}Al_{11}Zn$). The β phase $Mg_{17}Al_{11}Zn$ should be relatively unattacked within the alloy. The extent of the phenomenon (galvanic corrosion) is connected to the surface ratio between the cathodic β phase and the anodic α-phase. This is very low for the semi-solid cast alloy as compared with the die-cast alloy.[34,51-53]

Potentiodynamic polarization curve measurements in 0.17 mol/1 NaCl solution saturated with $Mg(OH)_2$ were carried out to analyze the electrochemical behavior of thin wall Mg prod-

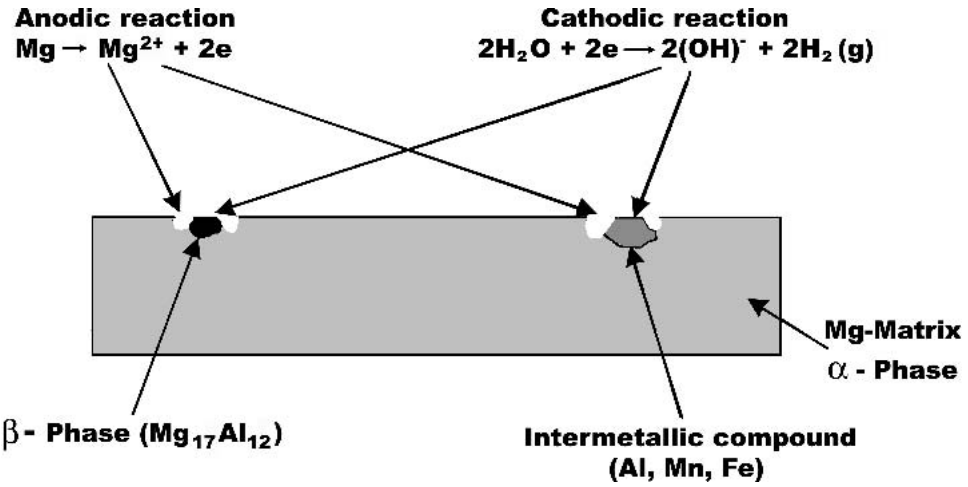


**Fig. 5** Schematic presentation of typical possible galvanic corrosion between some of the phases of Mg-Al alloys

ucts including commercial housings. It was found that the thixomolded and die-cast surfaces tend to be enriched with Al and the former was more prominent. The good corrosion resistance of thixomolded AZ91D was electrochemically verified by the presence of pseudo-passivation in NaCl solution. The passivation is considered as more stable at small $i_{pass}$ (passive current) with noble $E_{bd}$ (breakthrough potential). The test plate with 1 mm thickness seems to create the most stable surface. The decrease of section thickness is effective in improving the corrosion resistance. The corrosion rate of 0.018 MCD (mg/cm$^2$day) was obtained at a site, 0.8 mm thickness, according to ASTM B117 after 360 ks. Further decrease tends to provoke the localized corrosion near the overflow section. The selection of optimum wall thickness is useful for the production yields as well as corrosion resistance.[54,55] A significant statement relevant to the improvement of passivity can be attributed to the amorphous structure and the beneficial effect of NiO and $Nd_2O_3$ (for $Mg_{65}Ni_{20}Nd_{15}$).[56] Krishnamurthy et al.[57] noted a pseudo-passive behavior in rapidly solidified binary Mg-Nd alloys, and this was attributed to the modified passive layer enriched in Nd.[56,57] An improvement of corrosion behavior can be expected by the formation of another oxide in MgO or through the formation of a double oxide to give a continuous and uniform coverage of the alloy surface under various corrosion conditions.[58-60] It has been shown that the dissolution rates, determined from the volume increase of collected H gas of melt-spun amorphous Mg-Ni-Nd alloys immersed in 3% NaCl solution, were all much lower than that of pure Mg ribbon. $Mg_{65}Ni_{20}Nd_{15}$ exhibited a dissolution rate as low as 965.2 μm/y (38 mpy) in 3% NaCl solution saturated with $Mg(OH)_2$.[61] Using DP-XPS, Yao et al.[56] ascribed the high corrosion resistance of $Mg_{65}Ni_{20}Nd_{15}$ in 3% NaCl solution saturated with $Mg(OH)_2$ to the formation of a protective surface film with high content of oxidized Nd. Using AES depth profile, Gebert et al.[62] attributed the improved corrosion properties of amorphous $Mg_{65}Cu_{25}Y_{10}$ in high alkaline hydroxide electrolyte to the formation of a homogeneous, dense and highly protective passive film. It was reported that some $CO_3^{-2}$ species have been identified in the breakdown film, indicating that the incorporation of $CO_3^{-2}$ leads to a poor protection of the Mg surface.[59,63]

### 4.4 Skin Properties of Castings

The skin for cast materials of AZ 91D has been shown to have almost 10% of the corrosion current of the same polished interior material in 1 N NaCl at pH 11. The penetration rate in mm/y for the interior was 5.72 as compared with 0.66 of that of the surface, with the difference in corrosion rate being nearly a factor of 10 for corrosion rates in NaCl solutions.[64] The fine grain microstructure, the high volume fraction and nearly continuous nature of the intergranular β-$Mg_{17}Al_{12}$ in the near surface microstructure can result in the formation of an effective barrier against further corrosion.[5] There were also more micropores and the pores were somewhat larger in the center of the samples than towards the sample surfaces. Back-scattered SEM images showed that there was much more β phase and the β phase was finer in the skin layer of die-cast AZ91D than in the sample center.[5,64]

The β phase serves a dual purpose in corrosion; the β phase can act either as a barrier or as a galvanic cathode. When it has a beneficial effect to increase the corrosion resistance, the β phase is stable in the test solution and it is inert to corrosion attack. So, if the α grains are very fine and the β fraction is not too low, the β phase is nearly continuous like a net over the α matrix, and the β phase particles do not easily fall out by undermining. The corrosion of the α-phase is then quite easily obstructed by corrosion products on its surface, and so corrosion is greatly retarded. The high density of porosity in the center of the sample gives a larger exposed area to corrosion. The electrochemical processes inside of a micro-pore are easily obstructed by corrosion products and corrosion is accelerated by the auto-catalytic pitting mechanism, assisted also by the fact that the micro-pores usually originate from defects in the alloy.[64]

### 4.5 Welding and Localized Corrosion

Welded Mg structures and localized corrosion, and stress corrosion cracking (SCC) residual stresses heated by welding, are found particularly dangerous to SCC resistance and so a low-temperature thermal stress-relief is a recommended practice. Shot peening and other mechanical processes that create

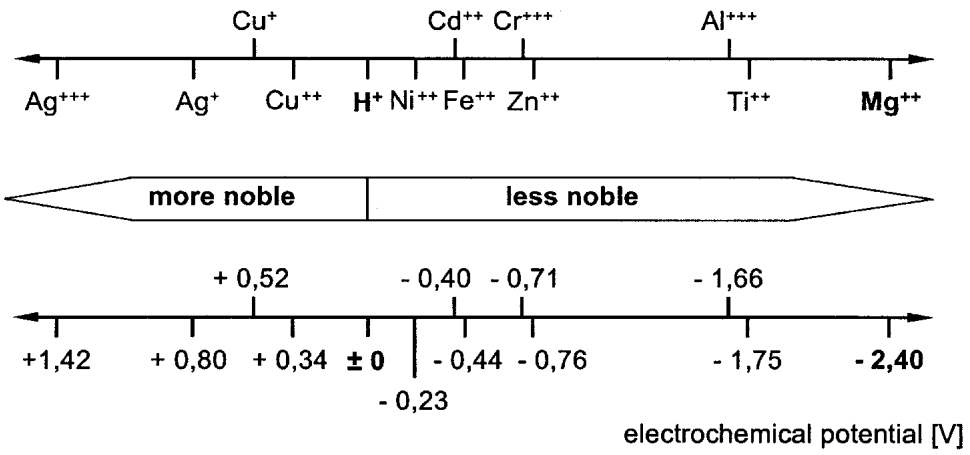


**Fig. 6** Standard reduction potentials of various metals

favorable compressive surface residual stresses may also increase SCC resistance.[2,28] Magnesium extruded alloys with approximately 3-8% Al and 0.5-0.8% Zn are susceptible to filiform corrosion and pitting corrosion in aqueous chloride solutions depending on the chloride concentration. The resistance of non-welded alloys increases with Al content. On welding of the alloys, the corrosion resistance is determined by the Al/Mg proportion at the surface of the non-affected material and the laser-welding seam. The pits occur mainly in the heat-affected zone of the welding seam. The laser beam welded material AZ61HP was found to have excellent resistance.[65]

## 5. Localized Corrosion Phenomena

### *5.1 Galvanic Corrosion*

Galvanic corrosion can start as general corrosion that can change to localized corrosion, and in other instances, it can begin as local galvanic attack depending on the metallic phase distribution and morphology, solution properties, agitation profile, temperature, etc. Since Mg is anodic (or sacrificial) to all other engineering metals, the severe corrosive attack that often occurs with Mg assemblies in salt water environments has long been a deterrent to the use of Mg alloys in structural applications. The degree to which the corrosion of Mg is accelerated by the galvanic couple in a given environment depends in part on the relative positions of the two metals in the electrochemical series (Fig. 6). Practical free corrosion potentials in a chloride-containing medium are given to show a more realistic estimation on the possible electromotive galvanic cell in a conducting medium (Fig. 7). Equally important is the polarization that reduces the potential difference of the couple as the galvanic current develops. Because Mg shows little, if any, anodic polarization in salt water, the reduction of the potential difference in the galvanic cell typically results from polarization of the cathode, where water is reduced to H gas and hydroxyl ions. Some metals, such as Fe, nickel (Ni), and copper (Cu) serve as efficient cathodes, while other metals, such as Al, Zn, cadmium (Cd), and tin (Sn), while equally cathodic to Mg in some environments, are much less effective cathodes due to their tendency to inhibit the combination of atomic H on surfaces to form the hydrogen gas that evolves.

Galvanic corrosion of Mg alloys can generally be attributed to two basic causes: (a) poor alloy quality due to excessive levels of heavy metal or flux contamination and (b) poor design and assembly practices, which can result in severe galvanic corrosion attack. For continuous outdoor use, where Mg assemblies may be wet or subjected to salt splash or spray, precautions against galvanic attack must be taken. Although corrosive attack from any source can jeopardize the satisfactory performance of Mg components, attack resulting from galvanic corrosion is probably the most detrimental. Improved performance in assemblies can be realized only if proper measures are taken to control the potential for galvanic attack through careful design, selection of compatible materials, and the selective use of coatings, sealants, and insulating materials. Under stagnant conditions of corrosion or under conditions of high cathodic current density where the pH becomes strongly alkaline, both the Mg and an amphoteric contacting metal such as Al may suffer severe attack. Al alloys containing appreciable Mg, such as 5052, 6053, and 5056, are least severely attacked in chloride media when galvanically coupled. This fact was observed in galvanic couples of Mg and Al alloys exposed to tide water and in the atmosphere at Hampton Roads, Virginia.[24]

Although the general corrosion resistance of high-purity Mg alloys is even better than A380 Al alloy in atmospheric or saline environments, galvanic corrosion remains a concern for design and applications engineers in developing Mg components. The poor corrosion resistance of many Mg alloys is mainly due to the internal galvanic corrosion caused by second phases or impurities. The degree of external galvanic corrosion attack on Mg is strongly influenced by the compatibility of the second metal in contact with the Mg parts, with Al alloy 5052 being the most compatible metal and steel the least. Proper design, combined with the use of non-conductive or compatible Al shims or washers, is a very simple and efficient way to prevent galvanic corrosion when a Mg part is attached to another metal.[4]

Galvanic corrosion can start as general corrosion that can transition to localized corrosion, and in several cases, it can begin as local galvanic attack depending on the metallic phase distribution and morphology, solution properties, agitation, and temperature. Common impurities that influence corrosion in commercial Mg alloys are Fe, Ni, Cu, Pb, and Si, and the

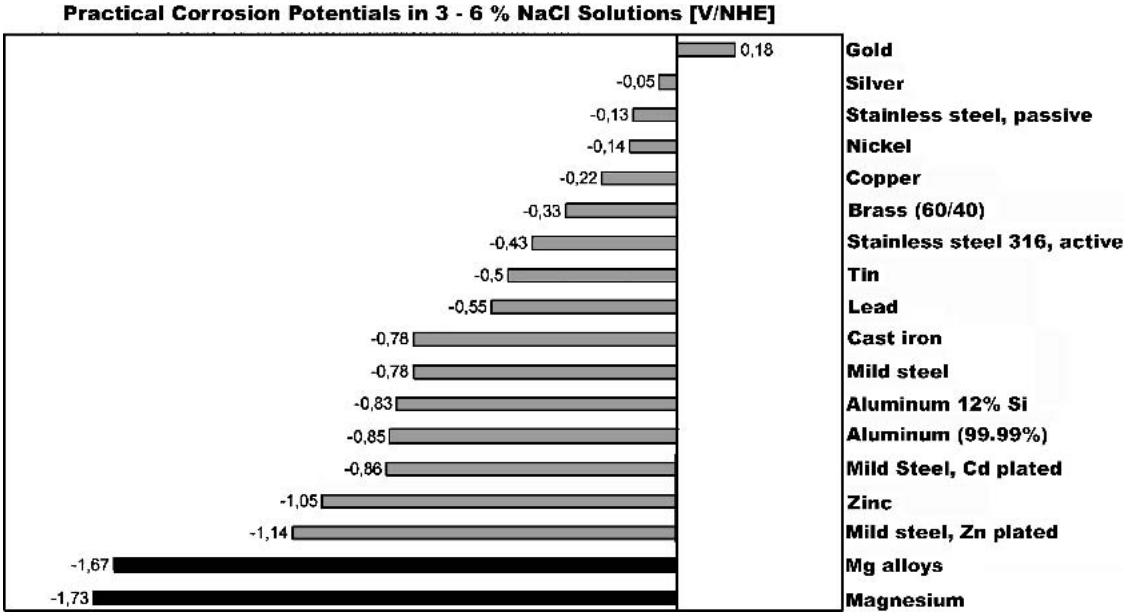


**Fig. 7** Practical corrosion potentials of various metals and alloys measured in 3-6% sodium chloride solution[29]

important Mg alloys containing Al, Mn and Zn. A general pitting attack is observed when Fe, Ni, or Cu content is in excess of the tolerance limit for one or more of the aforementioned elements. Blast residues such as steel from shot blasting or silica from sand blasting can cause general pitting attack in saline environments. Flux inclusions result in localized attack that is clustered or distributed randomly on machined surfaces of castings. Scanning electron microscopy/energy dispersive x-ray analysis of a freshly machined surface (free of fingerprints or other sources of contamination) reveal pockets of Mg and potassium (K) chlorides, as well as traces of Ca, Ba, and S. Zr and Zr-Fe compounds may also be associated with the deposits in Zr bearing alloys. Chromic acid pickling followed by chemical treatment and surface sealing can alleviate the problem of galvanic corrosion related to inclusions in finished castings. The use of sulfur (S) hexafluoride ($SF_6$) that replaces the fluxes for the protection of melts during casting can also be used to eliminate this problem.

The increase in corrosion rate due to Cu or Fe above their respective tolerance limits is considerably reduced by the presence of Mn or Zn. Zn also increases the tolerance limit of Mg to Ni. The use of 0.2-2% Mn and 1-1.5% Zn are indicated since they correspond actually to the present common alloys. The tolerance limits of these impurities have no explicit one reason till now, however, the four reasons given by Hanawalt et al. are[38]

- The limit of solubility of the impurity in the alloy can explain the tolerance limit of Cu impurity but not that of Fe.
- It can be admitted that isolated spots are not effective unless there are a critical number of cathodic sites to create an important attack.
- The absolute magnitude of the critical concentration depends upon the extent of corrosion caused about each particle. Probably, corrosion continues until the particle is removed by undermining itself.
- It is possible that there exists a critical anodic current density that will permit the film to form on the surface.

Severe corrosion may occur in neutral solutions of salts of heavy metals, such as Cu, Fe, and Ni. Such corrosion occurs when the heavy metal, the heavy metal basic salts, or both plate out to form active cathodes on the anodic Mg surface. This can be considered as galvanic corrosion that leads typically to localized corrosion such as pitting. Chloride solutions usually break down the protective film while fluoride solutions form insoluble Mg fluoride and corrosion is reduced. Oxidizing salts, containing chlorine (Cl) or S atoms, are more corrosive than non-oxidizing salts. Chromates, vanadates, phosphates, and many others are film forming and thus retard corrosion, except at elevated temperatures.

### *5.2 Pitting and Filiform Corrosion*

Pitting and crevice corrosion are usually associated with the breakdown of passivity. Filiform corrosion was observed at critical concentrations before that of pitting. Pitting is a form of localized corrosion that is often a concern in applications involving passivating metals and alloys in aggressive environments. Pitting can also occur in nonpassivating alloys with protective coatings or in certain heterogeneous corrosive media ASM.[36]

The AZ, AS, and AM type alloys maintain a bright and shiny appearance in the unattacked part of the corroded surface, whereas the AE alloys tend to become dull due to the build-up of a relatively thick hydroxide film and the formation of numerous small pits, usually only a few micrometers in depth. The corresponding backscattered electron image (BEI) and x-ray maps indicate a high chloride concentration in the

pits and high Al concentration in the unpitted areas. The few studies of pitting of Mg and Mg alloys have been concerned with comparing the pitting behavior of cast to that of rapidly solidified Mg alloys. In these studies, two parameters indicative of pitting resistance were measured: (a) $i_p$, the passive current density, which is a measure of the protective quality of the passive film, and (b) $E_b$, the breakdown potential, which indicates the resistance to the breakdown of the passive film that results in pitting attack. The more positive the value of $E_b$, the more protective is the film on the metal surface.[28]

Filiform corrosion tests for pitting and filiform corrosion were performed both in unstirred solutions and by exposure in a flow channel equipped with an optical cell for in situ microscopic observation of the corroding surface. These tests consisted of exposing the specimens to NaCl solutions of various concentrations at room temperature, 5% NaCl in most cases. Both de-aerated solutions and solutions exposed to ambient conditions were used.[66]

Filiform corrosion observed on AZ91 is quite different in nature from the well-known mechanisms of filiform corrosion and occurs on an uncoated surface with unusually high filament propagation velocities. This is very possibly due to the presence of a highly resistant air-formed oxide on alloy AZ91. Filiform propagation does not require the presence of dissolved oxygen in the environment; it is essentially fuelled by H evolution occurring at the filament head and outside the filaments. Anodic polarization enhances filiform corrosion at the expense of pitting. The rate of filament propagation is independent of material temper, surface treatment and presence of oxygen in the environment. It is controlled by mass transfer limitations resulting from the formation of a salt-film at the filament tip.[66]

Filiform corrosion is thought to be a special form of tunneling, which appears to be the forerunner of regular pitting. Filiform propagation is characterized by unusually high corrosion rates under high anodic control at the surface. Morphology and directionality of filaments are determined by the material microstructure such as compositional and crystallographic factors.[66] Filiform corrosion was observed in the uncoated AZ31, while general corrosion mainly occurred in the deposition coated AZ31, which seems to be suppressed during the preceding immersion test. Morphologies and compositions of corrosion products formed on the uncoated and deposition coated AZ31 alloy are different from one another, which is believed to lead to the difference in corrosion behavior.[67]

### 5.3 Crevice Corrosion

It is recognized that the environment within the crevice is different from that of the bulk environment. O differential cells could be established between cathode surfaces exposed to, for example, oxygenated seawater and anodic crevice areas. It could also be admitted that hydrolysis reactions within crevices could produce changes in pH and chloride concentration in the crevice environment. It is very probable that crevice corrosion can be initiated due to the hydrolysis reaction in case of Mg and Mg alloys, at least in certain conditions where it is believed that oxygen does not play a major role in the corrosion mechanism. The formation of Mg hydroxide should influence the properties of the interface between the Mg and the solution in the crevice.

It should be mentioned that in stagnant distilled water, Mg and Mg alloys have a very low rate of corrosion. It is important then to characterize water chemistry such as: pH, aeration, temperature, alkalinity, and specific dissolved ion concentrations. Contaminants may vary as a function of the source (well, river, estuary, storm drains) and of climatic conditions (wind direction, temperature, acid rain). Any heavy metal contamination of the aqueous solution at the interface can plate out on the metal surface and cause galvanic localized attack. Natural waters, depending on the source, may have variable concentrations of dissolved carbonates such as Ca, Mg, and/or Na, with the solubility controlled by the partial pressure of C dioxide and the solubility product of Ca carbonate that vary with alkalinity and temperature.[36]

## Acknowledgments

Thanks are given to Dr. Norbert Hort from GKSS for fruitful discussions and M. Pierre Gelinas, B.Sc. in metallurgical engineering for revision and help.

## References

1. Anon., Technical communication, Dow Chemical Company, Dow North America, Freeport, TX, 1994, 77541.
2. W.K. Miller and E.F. Ryntz, Jr.: "Magnesium for Automotive Applications. A State-of-the-Art Assessment, Localized Corrosion," Society of Automotive Engineers, Warrendale, PA, 1984, p. 2.524-2.542.
3. E. Aghion, B. Bronfin, F. Von Buch, S. Schumann, and H. Friedrich: "Dead Sea Magnesium Alloys Newly Developed for High Temperature Applications" in *Magnesium Technology 2003,* H.I. Kaplan, ed., The Minerals, Metals & Materials Society, Warrandale, PA, 2003, pp. 177-82.
4. A. Luo, M. Balogh, and B.R. Powell: "Tensile Creep and Microstructure of Magnesium-Aluminum-Calcium Based Alloys for Powertrain Applications: Part 2 of 2," SAE Paper No. 2001-02-0423, SAE, Warrendale, PA, 2001.
5. G.L. Dunlop, W.P. Sequeira, M.S. Dargusch, G. Song, A. Atrens, T. Kittel, D. St. John, A.K. Dahle, and M. Murray: "Microstructure and Properties of Magnesium DIE Casting" in *Proceedings of the 1998 Annual World Magnesium, A Global Vision for Magnesium,* 55th meeting of the International Magnesium Association, ed., May 1998, Coronado, CA, International Magnesium Association, McLean, VA, 1998, pp. 68-73.
6. M. Pekguleryuz and E. Baril: "Development of Creep Resistant Mg-Al-Sr Alloys" in *Magnesium Technology 2001,* J. Hryn, ed., The Minerals, Metals & Materials Society, Warrendale, PA, 2001, pp. 119-25.
7. M. Pekguleryuz, P. Labelle, D. Argo, and E. Baril: "Magnesium Alloy AJ62X with Superior Creep Resistance, Ductility and Die Castability" in *Magnesium Technology 2003,* H.I. Kaplan, ed., The Minerals, Metals & Materials Society, Warrendale, PA, 2003, pp. 201-206.
8. K. Pettersen, H. Westengen, J.I. Skar, M. Videm, L-Y. Wei: "Creep Resistant Mg Alloy Development" in *Magnesium Alloys and Their Applications,* K.U. Kainer, ed., WILEY-VCH Verlag GmbH, Germany, 2000, pp. 29-34.
9. B.R. Powell, A.A. Luo, V. Rezhets, J.J. Bommarito, and B.L. Tiwari: "Development of Creep-Resistant Magnesium Alloys for Powertrain Applications: Part 1 of 2," SAE Technical Paper 2001-01-0422, SAE, Detroit, MI, 2001.
10. P. Lyon, J.F. King, and K. Nuttal: "A New Magnesium HPDC Alloy for Elevated Temperature Use" in *Proceedings of the Third International Magnesium Conference,* G. W. Lorimer, ed., The Institute of Materials, Manchester, UK, 1996, pp. 99-108.
11. J. Mason and R.T.W Clyne, in A.R. Bunsell, P. Lamicq and A. Massiah (ed.), Proc. 3rd European Conference on Composite Materials (ECCM3), France, 20-23 March 1989, Elsevier, Amsterdam, 1989, p. 213.

12. C. Jaschik (Sp), H. Haferkamp, and M. Niemeyer: "New Magnesium Wrought Alloys" in *Magnesium Alloys and Their Applications,* K.U. Kainer, ed., WILEY-VCH Verlag, Germany, 2000, pp. 41-46.
13. A. Sanschagrin, R. Tremblay, R. Angers, and D. Dubé: "Mechanical Properties and Microstructure of New Magnesium-Lithium Base Alloys," *J Mater Sci Eng,* 1996, A220, pp. 69-77.
14. I.J. Polmear: "Magnesium Alloys and Their Application," *Mater. Sci. Technol.,* 1994, *10*(1), pp. 1-6.
15. R.L. Edgar: "Global Overview on Demand and Applications for Magnesium Alloys, International Congress" in *Magnesium Alloys and Their Applications,* K.U. Kainer, ed., WILEY-VCH, Weinheim, Germany, 2000, pp. 3-8.
16. P. Bakke, K. Pettersen, and H. Westengen: "Enhanced Ductility and Strength Through RE Addition to Magnesium Die Casting Alloys" in *Magnesium Technology 2003,* H.I. Kaplan, ed., The Minerals, Metals & Materials Society, Warrendale, PA, 2003, pp. 171-76.
17. D.M. Walukas, R.F. Decker, R.E. Vining, and R.D. Carnahan: "Thixomolding® of Magnesium" in *Magnesium 97 Proceedings of the First Israeli International Conference on Magnesium Science & Technology,* E. Aghion and D. Eliezer, ed., Magnesium Research Institute Ltd., Beer-Sheva, Israel, 1977, pp. 54-59.
18. R. Beals, S. LeBeau, O. Roberto and P. Shashkov: "Advances in Thixomolding Magnesium Alloys Part II, 2003," in *Magnesium Technology 2003,* H.I. Kaplan, ed., TMS (The Minerals, Metals & Materials Society), The Minerals, Metals & Materials Society, Warrendale, PA, pp. 283-88.
19. H. Kaufmann and P.J. Uggowitzer: "The Fundamentals of the New Rheocasting Process for Magnesium Alloys," in *Magnesium Alloys and their Applications Proceedings,* K.U. Kainer, ed., Wiley-VCH, Weinheim, Germany. 2000, pp. 533-39.
20. W. Fragner, C. Peterlechner, and R. Potzinger: "Scale-up of Magnesium New Rheocasting from a Laboratory Level to an Industrial Process" in *Magnesium Technology 2003,* H.I. Kaplan, ed., The Minerals, Metals & Materials Society, Warrendale, PA, 2003, pp. 277-82.
21. H. Kaufmann, R. Potzinger, and P.J. Uggowitzer: "NRC – Magnesium Castings for Structural Applications" in *Met. Soc., Light Metals 2001 Métaux Légers, COM 2001,* M. Sahoo and T.J. Lewis, ed., Canadian Institute of Mining, Metallurgy and Petroleum, Quebec, Canada, pp. 216-23.
22. M. Pourbaix, *Atlas of Electrochemical Equilibria in Aqueous Solutions,* NACE International and CEBELCOR (Centre Belge d'Étude de la Corrosion), Houston, TX, 1974, p. 141.
23. G. G. Perrault: "Magnesium," in *Encyclopedia of Electrochemistry of the Elements,* A.J. Bard, ed., Vol. VIII, Marcel Dekker, NY, 1978, Chap. VIII-4, pp. 262-318.
24. A.F. Froats, T.Kr. Aune, D. Hawke, W. Unsworth, and J. Hillis: "Corrosion of Magnesium and Magnesium Alloys," in *Metals Handbook,* 9th ed., Corrosion ASM International, Materials Park, OH, 1987, Vol. 13, pp. 740-54.
25. D.L. Hawke, J.E. Hillis, M. Pekguleryuz, and I. Nakatsugawa: "Corrosion Behavior," in *Magnesium and Magnesium Alloys,* M. M. Avedesian and H. Baker, ed., ASM International, Materials Park, OH, 1999, pp. 194-210.
26. N.S. McIntyre and C. Chen: "Role of Impurities on Mg Surfaces Under Ambient Exposure Conditions," *Corrosion Science,* 1998, *40* (10), pp. 1697-1709.
27. J.H. Nordlien, S. Ono, N. Masuko, and K. Nisancioglu: "Morphology and Structure of Oxide Films Formed on Magnesium by Exposure to Air and Water, *J. Electrochemical Soc.,* 1995, *142*(10), pp. 3320-22.
28. E. Ghali: "Magnesium and Magnesium alloys" in *Uhlig's Corrosion Handbook,* R.W. Revie, ed., John Wiley, New York, 2000, Ch. 44, pp. 793-830.
29. G.L. Song and A. Atrens: "Corrosion Mechanisms of Magnesium Alloys," *Adv. Eng. Mater.,* 1999, *1*(1), pp. 11-33.
30. G.L. Song, A. Atrens, and M. Dargusch: "Influence of Microstructure on the Corrosion of Diecast AZ 910," *Corros., Sci.,* 1999, *41,* pp. 249-73.
31. J.H Nordlien., K. Nisancioglu, S. Ono, and N. Masuko: "Morphology and Structure of Oxide Films Formed on MgAl Alloys by Exposure to Air and Water," *J. Electrochem. Soc.,* 1996, *143*(8), pp. 2654-72.
32. W.A. Ferrando: "Review of Corrosion and Corrosion Control of Magnesium Alloys and Composites," *J. Mater. Eng.,* 1989, *11*(4), pp. 299-313.
33. J.E. Hillis: "Magnesium" in *Corrosion Testing and Standards: Application and Interpretation,* ASTM Manual Series: MNL 20, R. Baboian, ed., ASTM, Philadelphia, PA, 1995, Ch. 45, pp. 438-46.
34. S. Mathieu, C. Rapin, J. Hazan, and P. Steinmetz: "Corrosion Behavior of High Pressure Die-Cast and Semi-Solid Cast AZ91D Alloys," *Corrosion Science,* 2002, *44,* pp. 2737-56.
35. G.L. Makar and J. Kruger: "Corrosion Studies of Rapidly Solidified Magnesium Alloys," *J. Electrochem. Soc.,* 1990, *137,* pp. 414-21.
36. C.H. Baloun: "Corrosion Testing in Water," in *Corrosion,* ASM, Metals Handbook, 9th ed., ASM International, Materials Park, OH, 1987, Vol. 13, pp. 207-208.
37. B-Y. Hur, and K-W. Kim: "A New Method for Evaluation of Pitting Corrosion Resistance of Magnesium Alloys," *Corrosion Rev,* 1998, *16*(1-2), pp. 85-94.
38. J.D. Hanawalt, C.E., Nelson, and J.A. Peloubet: "Corrosion Studies of Magnesium and Its Alloys," *Trans. Am. Soc. Mining Metall. Eng.,* 1942, *147,* pp. 273-99.
39. J.L. Robinson, and P.F. King: *J. Electrochem. Soc.,* 1961, *108,* pp. 36-41.
40. G. Baril, and N. Pebere: "The Corrosion Behavior of Pure Magnesium in Aerated and De-Aerated Sodium Sulfate Solution," *Corrosion Science,* 2001, *43,* pp. 471-84.
41. F. Czerwinski: "The Oxidation of Magnesium Alloys in Solid and Semisolid States" in *Magnesium Technology 2003,* H.I. Kaplan, ed., The Minerals, Metals & Materials Society, Warrendale, PA, 2003, pp. 39-42.
42. O. Lunder, K. Nisancioglu, and R.S. Hansen: "Corrosion of Die Cast Magnesium-Aluminum Alloy," Congress and Exposition, Paper No. 930755, SAE, Detroit, MI, Society of Automotive Engineering, Inc., Warrendale, PA, pp. 117-126.
43. V. Mitrovic-Scepanovic and R.J. Brigham: "Localized Corrosion Initiation on Magnesium Alloys," *Corrosion,* 1992, *48*(9), pp.780-84.
44. S.J. Splinger and N.H. McIntyre: "The Initial Interaction of Water Vapour with Mg-Al Alloy Surfaces at Room Temperature," *Surf. Sci.,* 1994, *314,* pp. 157-71.
45. T. Beldjoudi, C. Fiaud, and L. Robbiola: "Influence of Homogenization and Artificial Aging Heat Treatments on Corrosion Behavior of Mg-Al Alloys," *Corrosion,* 1993, *49,* pp. 738-45.
46. M.J. Danielson and R.H. Jones: "The Interaction Between Microstructure and Corrosion Initiation in Certain Die Cast and Thixomolded® Magnesium Alloys" in *Magnesium Technology 2001,* J. Hryn, ed., The Minerals, Metals & Materials Society, Warrendale, PA, 2001, pp. 263-68.
47. P.Y. Li, H. J. Yu, S.C. Chen, and Y.M. Yu: "Factors Affecting the Corrosion Resistance of Cast Magnesium Alloys" in *Magnesium Technology 2003,* H.I. Kaplan, ed. The Minerals, Metals & Materials Society, Warrendale, PA, 2003, pp. 51-58.
48. B.R. Powell, A.A. Luo, B.L. Tiwari, and V. Rezhets: "The Die Castability of Calcium-Containing Magnesium Alloys: Thin-Wall Computer Case" in *Magnesium Technology 2002,* H.I. Kaplan, ed., The Minerals, Metals & Materials Society, Warrendale, PA, 2002, pp. 123-29.
49. B.L. Tiwari and J.J. Bommarito: "A Novel Technique to Evaluate the Corrosion Behavior of Magnesium Alloys" in *Magnesium Technology 2002,* H.I. Kaplan, ed., The Minerals, Metals & Materials Society, Warrendale, PA, 2002, pp. 269-75.
50. C. Chen, S.J. Splinter, T. Do, and N.S. McIntyre: "Measurement of Oxide Film Growth on Mg and Al Surfaces Over Extended Periods Using XPS," *Surf. Sci.,* 1997, *382,* p. L652-L657.
51. P.L. Bonora, M. Andrei, A. Eliezer, E.M. Gutman: "Corrosion Behavior of Stressed Magnesium Alloys," *Corrosion Sci.*, 2002, *44,* pp. 729-49.
52. O. Lunder, T.Kr. Aune, and K. Nisancioglu: "Effect of Mn Additions on the Corrosion Behavior of Mould-Cast Magnesium ASTM AZ91," *Corrosion,* 1987, *43,* pp. 291-95.
53. D. Daloz, P. Steinmetz, and G. Michot: "Corrosion Behavior of Solidified Magnesium-Aluminum-Zinc Alloys," *Corrosion,* 1993, *53*(12), pp. 944-54.
54. I. Nakatsugawa, H. Takayasu, and K. Saito: "Corrosion Behavior of Thin Wall Magnesium Products Molded by Thixomolding, Magnesium Alloys and Their Applications" in *Magnesium Alloys and Their Applications,* K.U. Kainer, ed., WILEY-VCH Verlag, Weinheim, Germany, 2000, pp. 445-50.

55. I. Nakatsugawa, F. Yamada, H. Takaysu, T. Tsukeda, and K. Saito: "Corrosion Behavior of Thixomolded Mg-Al Alloys" in *Proceedings 38th Annual Conference METSOC, CIM, Environmental Degradation of Materials and Corrosion Control in Metals,* M. Elboujdaini and E. Ghali, ed, Canadian Institute of Mining, Metallurgy and Petroleum, Quebec, Canada, 1999, pp. 113-23.
56. H.B. Yao, Y. Li, A.T.S. Wee, J.S. Pan, and J.W. Chai: *Surf. Rev. Lett.,* 2001, *8*(5), p. 575.
57. S. Krishnamurthy, M. Khobaib, E. Robetson, and F.H. Froes: "Corrosion Behavior of Rapidly Solidified Mg-Nd and Mg-Y Alloys," *Mater. Sci. Eng.,* 1988, *99,* pp. 507-11.
58. E.A. Shaw, R.M. Ormerod, and R.M. Lambert: "Oxidation of Neodymium Overlays and Nd/Cu Alloy Films on Cu(111): Observation of Chemisorbed Oxygen on Top of $Nd_x$/Cu(111)," *Surf. Sci.* 1992, *275,* pp. 157-69.
59. H.B. Yao, Y. Li, A.T.S. Wee, J.W. Chai, and J.S. Pan: "Correlation Between Corrosion Behavior and Corrosion Films Formed on the Surfaces of $Mg_{82-x}Ni_{18}Nd_x$ (x = 0, 5, 15) Amorphous Alloys," *Appl. Surf. Sci,* 2001, *173,* pp. 54-61.
60. H.B. Yao, Y. Li, A.T.S. Wee, J.W. Chai, and J.S. Pan: "The Alloying Effect of Ni on the Corrosion Behavior of Melt-spun Mg-Ni Ribbons," *Electrochim. Acta,* 2001, *46,* p. 2649-57.
61. C.H. Kam, Y. Ki, S.C. Ng, A.T.S. Wee, J.S. Pan, and H. Jones: "The Effect of Heat Treatment on the Corrosion Behavior of Amorphous Mg-Ni-Nd Alloys," *J. Mater. Res.* 1999, *14*(4), pp. 1638-44.
62. A. Gebert, U. Wolff, A. John, J. Eckert, and L. Schultz: "Stability of the Bulk Glass-Forming $Mg_{65}$ $Y_{10}$ $Cu_{25}$ Alloy in Aqueous Electrolytes Materials," *Mater. Sci. Eng.* 2001, *A299,* pp. 125-35.
63. C.B. Baliga and P. Tsakpoulos: "Development of Corrosion-Resistant Magnesium Alloys 1. Characterization of Splat Quenched Mg-10Al and Mg-16Al," *Mater. Sci. Technol.,* 1993, *9,* pp. 507-11.
64. G.L. Song, and A. Atrens: "Corrosion Behavior of Skin Layer and Interior of Die Cast AZ91D" in *Magnesium Alloys and Their Applications,* Proc. Fourth Intl. Conf. on Magnesium Alloys and Their Applications, Wolfsburg, Germany, B.L. Mordike and K.U. Kainer ed., Werkstoff-Informationsgesellschat, Frankfurt, Germany, 1998, pp. 415-19.
65. K. Lübbert, J.Kopp, and E. Wendler-Kalsch: "Corrosion Behavior of Laser Beam Welded Aluminum and Magnesium Alloys in the Automotive Industry," *Mater. Corrosion,* 1999, *50,* pp. 65-72.
66. O. Lunder, J.E. Lein, S.M. Hesjevik, T.K. Aune, and K. Nisancioglu: "Corrosion Morphologies on Magnesium Alloy AZ91," *Werkstoffe und Korrosion* 1994, *45,* pp. 331-40.
67. A. Yamamoto, A. Watanabe, K. Sugahara, S. Fukumoto, and H. Tsubakino: "Applying a Vapor Deposition Technique to Improve Corrosion Resistance in Magnesium Alloys" in *Proceedings of the Second International Conference on Environment Sensitive Cracking and Corrosion Damage,* M. Matsumura, H. Nagano, K. Nakasa, and Y. Isomoto, ed., Nishiki Printing Ltd, ESCCD 2001, Hiroshima, Japan, 2001, pp. 160-67.